



## Open Archive Toulouse Archive Ouverte

OATAO is an open access repository that collects the work of Toulouse researchers and makes it freely available over the web where possible

This is an author's version published in: <https://oatao.univ-toulouse.fr/26496>

### Official URL :


<https://doi.org/10.1007/s10498-020-09386-8>

#### **To cite this version:**

Nkoue Ndong, Gustave Raoul and Probst, Jean-Luc and Ndjama, J. and Ndam Ngoupayou, Jules Remy and Boeglin, J.-L. and Takem, G. E. and Brunet, F. and Mortatti, J. and Gauthier-Lafaye, F. and Braun, J.-J. and Ekodeck, G. E. *Stable Carbon Isotopes  $\delta^{13}C$  as a Proxy for Characterizing Carbon Sources and Processes in a Small Tropical Headwater Catchment: Nsimi, Cameroon*. (2020) *Aquatic Geochemistry*, 26. 1-30. ISSN 1380-6165

Any correspondence concerning this service should be sent to the repository administrator: [tech-oatao@listes-diff.inp-toulouse.fr](mailto:tech-oatao@listes-diff.inp-toulouse.fr)

# Stable Carbon Isotopes $\delta^{13}\text{C}$ as a Proxy for Characterizing Carbon Sources and Processes in a Small Tropical Headwater Catchment: Nsimi, Cameroon

Gustave Raoul Nkoue Ndongo<sup>1</sup> · J.-L. Probst<sup>2</sup> · J. Ndjama<sup>4</sup> · Jules Remy Ndam Ngoupayou<sup>5</sup>  · L. Boeglin<sup>3</sup> · G. E. Takem<sup>4</sup> · F. Brunet<sup>2</sup> · J. Mortatti<sup>6</sup> · F. Gauthier-Lafaye<sup>7</sup> · J.-J. Braun<sup>3,4,8</sup> · G. E. Ekodeck<sup>5</sup>

## Abstract

Stream carbon fluxes are one of the major components in the global C cycle, yet the discrimination of the various sources of stream carbon remains to a large extent unclear and less is known about the biogeochemical transformations that accompany the transfer of C from soils to streams. Here, we used patterns in stream water and groundwater  $\delta^{13}\text{C}$  values in a small forested tropical headwater catchment to investigate the source and contribution from the soil carbon pools to stream organic and inorganic carbon behavior over seasonal scales. Stream organic carbon (DOC and POC) comes mainly from the upper rich soil organic carbon horizons and derived from total organic carbon (TOC) of biogenic source. The isotopic compositions  $\delta^{13}\text{C}_{\text{TOC}}$ ,  $\delta^{13}\text{C}_{\text{DOC}}$  and  $\delta^{13}\text{C}_{\text{POC}}$  of these carbon species were very close ( $-30\text{‰}$  to  $-26\text{‰}$ ) and typical of the forested C3 vegetation. The relationship observed between DOC and  $\log \text{pCO}_2$  and  $\delta^{13}\text{C}_{\text{DIC}}$  indicated that besides the considerable  $\text{CO}_2$  evasion that occurs as DIC is transported from soils to streams, there were also other processes affecting the stream DIC pool. In-stream mineralization of DOC and mixing of atmospheric carbon had a significant influence on the  $\delta^{13}\text{C}_{\text{DIC}}$  values. These processes which varied seasonally with hydrological changes represent the main control on DOC and DIC cycling in the wet tropical milieu. The rapid turnover of carbon on hillside soils, the transformation of TOC to DOC in wetland soils and further mineralization of stream DOC to DIC favor the evasion of C, making the zone a source of carbon to the atmosphere.

**Keywords** Dissolved inorganic carbon (DIC) ·  $\delta^{13}\text{C}$  carbon isotope composition · Dissolved organic carbon (DOC) · Soil organic carbon mineralization · Partial pressure of  $\text{CO}_2$  ( $\text{pCO}_2$ ) · Carbon sources

---

**Electronic supplementary material** The online version of this article (<https://doi.org/10.1007/s10498-020-09386-8>) contains supplementary material, which is available to authorized users.

✉ Gustave Raoul Nkoue Ndongo  
raoulnkoue@yahoo.fr

Extended author information available on the last page of the article

# 1 Introduction

Terrestrial carbon export via inland aquatic systems is a key process in the global carbon cycle that include sources of carbon to the atmosphere via outgassing from rivers and or reservoirs and carbon fixation in the water column as well as in sediments (Marx et al. 2017). Much studies on terrestrial carbon export balances have focus on large size rivers (Bird et al. 1998; Richey et al. 2002; Brunet et al. 2005; Crawford et al. 2014). However, much remains to be done with respect to headwater streams that are even very important because their biogeochemistry directly reflects carbon input from soil and groundwater (Amiotte-Suchet et al. 1999; Lambert et al. 2011; Huang et al. 2013; Campeau et al. 2018). The soil–stream interface is known to be a site for biogeochemical and physical transformation for the cycling of carbon and the major driver of terrestrial dissolved inorganic, organic and particulate organic carbon (DIC, DOC and POC) influxes (Öquist et al. 2009; Ledesma et al. 2017; Marx et al. 2017; Zhong et al. 2018). The close connectivity between soils and headwater streams therefore justifies much of their contribution to inland stream water carbon.

Soil organic carbon (SOC) is a main control on DOC and POC supply to headwater streams (Coynel et al. 2005; Lambert et al. 2014). Stream DOC and POC loads generally increase with increasing discharge, notably after the onset of precipitation (Morel et al. 2009; Brunet et al. 2009) because the rise in water table leads to the increase in runoff that leaches the soils. This is consistent with supply of SOC from topsoil horizons of wet-land areas, which is different from that of deeper hillside soil horizons (Billett et al. 2006; Evans et al. 2007; Sanderman et al. 2009; Lambert et al. 2014). DOC transport from soils to the stream network is governed by the interactions between soil carbon reservoirs and catchment hydrology (Lambert et al. 2011). A positive correlation has been found between stream DOC fluxes and the percentage of wetland area of headwater (Andersson and Nyberg 2008; Billett et al. 2006; Lauerwald et al. 2012). This relationship, which is consistent with flow regimes, justifies the correlation between DOC concentrations and the seasonal variability of stream discharge (Strohmeier et al. 2013). Mineralization of DOC to  $\text{CO}_2$  and DIC controls the fate of carbon from soils to stream networks (Palmer et al. 2001; Bengtson and Bengtsson 2007). Thus, stream  $\text{CO}_2$  and DIC concentrations are closely linked to DOC concentration patterns and compositions (Amiotte-Suchet et al. 2007; Brunet et al. 2009; Lapierre et al. 2013). Generally, DIC is considered the most abundant carbon specie in rivers and streams, mostly supplied by groundwater (Marx et al. 2017). DIC is made of the different inorganic carbon species ( $\text{CO}_{2(\text{aq})}$  and  $\text{H}_2\text{CO}_3$ ,  $\text{HCO}_3^-$  and  $\text{CO}_3^{2-}$ ) whose relative proportion in water depends on pH and temperature (Dickson et al. 2007). Hence, the relative distribution of DIC species in groundwater and streams is different in catchments with silicate (dominated by  $\text{CO}_{2(\text{aq})}$ ,  $\text{H}_2\text{CO}_3$  and  $\text{HCO}_3^-$ ) and carbonate bedrock (dominated by  $\text{CO}_3^{2-}$ ) (Ludwig et al. 1996). Water from catchments with strictly silicate basement can have pH values below 4.5, being oversaturated in  $\text{CO}_{2(\text{aq})}$  and leading to  $\text{CO}_2$  outgassing (Campeau et al. 2017; Zhong et al. 2018). This rapid evasion of soil-derived carbon dioxide to the atmosphere upon delivery to streams is the main contributor for the cycling of DIC (Brunet et al. 2009; Marx et al. 2017). Although  $\text{CO}_2$  exchange drives current understanding of DIC cycling between soils and headwater streams (Leith et al. 2015; Campeau et al. 2018), the relative contributions of DIC production processes remain generally unclear. In headwater streams, DIC originates mostly from soil-respired  $\text{CO}_2$  that is produced by root and microbial respiration, including the decomposition of organic matter (Amundson et al. 1998). The  $\text{CO}_2$  produced is involved in mineral weathering; thus, the

DIC export from headwater streams is strongly related to lithology (Probst et al. 1994; Telmer and Veizer 1999; Wallin et al. 2013). In-stream aquatic biodegradation and photodegradation (Opsahl and Zepp 2001; Porcal et al. 2015) and fixation of atmospheric CO<sub>2</sub> in headwater catchments may also regulate DIC and influence the interpretation of the DIC cycling (Marx et al. 2017; Campeau et al. 2018).

Previous studies have highlighted the fact that variable physical and biogeochemical mechanisms and hydrological connectivity control the carbon dynamics in headwater streams. These studies highlight the fact that water fluxes alone would not permit the understanding of seasonal changes of carbon dynamics in streams without taking into account the processes governing the transformation of carbon at the soil–stream interface. This interplay of biological, chemical and physical processes influencing carbon dynamics in headwater streams is, however, complex and often causes high spatiotemporal variability. Some studies (Feller and Beare 1997; Wynn et al. 2006) have used the stable C isotope ratio (<sup>13</sup>C/<sup>12</sup>C) to trace these different biogeochemical transformations in both stream water and groundwater. Studies on the variation of the DOC and POC isotopic signature in soil waters, groundwaters and stream waters have shown that the variation in the isotopic composition of SOM strongly influences that of DOC and POC (Lambert et al. 2011). The δ<sup>13</sup>C has been successfully used to distinguish between in situ aquatic production and soil-derived POC (Balakrishna and Probst 2005; Caroni et al. 2012). The interpretation of δ<sup>13</sup>C values of DIC in stream water and groundwater was successfully applied to distinguish between the biogenic and the geogenic source of DIC (Deines et al. 1974). δ<sup>13</sup>C<sub>DIC</sub> values have recently been considered a potential measure of the degree of atmospheric CO<sub>2</sub> evasion from groundwaters and streams (Polsenaere and Abril 2012; Venkiteswaran et al. 2014), but this patterns in δ<sup>13</sup>C<sub>DIC</sub> values simultaneously reflect a larger range of sources and processes (Campeau et al. 2017).

While several studies have used the δ<sup>13</sup>C values to interpret the organic and inorganic carbon dynamics in large river systems, few studies have focused on headwater systems (Amiotte-Suchet et al. 1999; Palmer et al. 2001; Doctor et al. 2008; Lambert et al. 2011, 2014; Campeau et al. 2018). Moreover, only few of these studies have been conducted in strictly silicate catchments where the influence of geogenic DIC sources can be ignored (Amiotte-Suchet et al. 1999; Campeau et al. 2018).

The Nsimi Small Experimental Watershed (NSEW) has been under investigation for hydrology and biogeochemistry for the last 20 years. This catchment is a local unit which forms part of the Nyong River Basin Network, the second largest river in Cameroon and one of the rare environmental observatory sites for climate and hydrochemical studies in the Central African tropical region. The close connectivity between soils and headwater streams justifies much of their contribution to inland stream water carbon at local scale and to the transfer of soil carbon to the ocean at regional scale. The NSEW is developed on a granito-gneissic basement and is under two geomorphologically controlled systems: (1) a hillside lateritic system and (2) a hydromorphic swamp system. Previous studies on hydrochemical transfer and water dynamics have provided knowledge on water pathways and outlined a hydrological model for the catchment. The mineralogy and geochemistry of the solid phases and the water chemistry have been extensively studied within both systems. (Ndam 1997; Olivie-Lauquet et al. 1999, 2000; Viers et al. 2000, 2001; Boeglin et al. 2003; Ndam Ngoupayou et al. 2005a; Braun et al. 2005; Maréchal et al. 2011). Flux studies have reported the organic carbon dynamics and contemporary fluxes for major (Ca, Na, Mg, K, Fe, Al, Ti) and for selected trace elements (Th, Zr) at the outlet of the NSEW (Viers et al. 1997; Olivia et al. 1999; Ndam Ngoupayou et al. 2005b; Braun et al. 2005). These studies showed that the organic-rich surface waters draining the swamp system, in which DOC

represented almost 50% of dissolved load, enhanced the mobilization and transfer of Al, Fe and transition metals such as Th, Ti and Zr (Braun et al. 2005). However, the contribution of each system to organic and inorganic carbon sources and the determination of factors controlling carbon chemistry and temporal changes in carbon pools with seasons remains poorly understood in this headwater catchment. Nkoue Ndong (2008) and Brunet et al. (2009) used the distribution of stable isotopes in river water to constrain and quantify the flux of organic and inorganic carbon from the river to the ocean and atmosphere. This study showed the role of swamps as source areas of DOC, but did not, however, highlight the native processes that link the soil carbon sources to stream carbon and their relative evolution throughout the hydrological cycle.

This study aims to use the  $\delta^{13}\text{C}$ , to link the vertical distribution of total organic carbon (TOC) in both ferrallitic and hydromorphic soil systems to groundwater and stream water DOC, POC and DIC, highlighting the biogeochemical processes that control the seasonal shift of carbon species in the catchment and their seasonal variation in response to hydrological changes.

The specific objectives were: (1) to trace the main sources of dissolved organic and inorganic carbon in the soil–stream system, (2) to investigate the processes that control the carbon transformation and (3) to ascertain the seasonal variation of different carbon components in order to assess the contribution of different carbon pools with hydrological changes.

## 2 SiteDescription

The 60 ha Nsimi Small Experimental Watershed (NSEW) is a first-order headwater catchment located in southern Cameroon (3° 10' N, 11° 51' E) and forms part of the Nyong river basin (Fig. 1). This site belongs to a long-term monitoring program of hydro-biogeochemical cycles within the rainforest of Central Africa, as part of the French network of Environmental Research Observatories (ORE), jointly set up and managed by the “Institut de Recherche pour le Développement” (IRD) and the “Centre National de la Recherche Scientifique” (CNRS) (Braun et al. 2005; Boeglin et al. 2005; Brunet et al. 2009).

NSEW is characterized by convexo-concave rounded hills that ranges from 669 m at the outlet to 703 m at the top of the hill, separated by flat swamps zone. Soils in the catchment have developed from granites and granitoid basement belonging to the Congo shield (Maurizot et al. 1986; Takam et al. 2009). The hillside regolith is composed of a 15-m-thick saprolite and complex polygenetic lateritic soil that consists of four main horizons, namely the mottled clay horizon, the carapace, the nodular ferruginous horizon and the soft clayey topsoil, which is overlain by a thin organic layer (Braun et al. 2005). The thickness of the soil cover decreases progressively toward the flat swamp, in which the poor drainage leads to the development of hydromorphic soils. A thick dark-brown organic-rich horizon composed of dead and living roots and other plant residues overlies the hydromorphic soils. Semideciduous rainforest covers 60% of the rounded hills, and cultivated food crops cover the remaining 40%. Semiaquatic plants of the Araceae family, *Gilbertiodendron dewevrei* and *Raffia monbuttorum* (raffia palm trees) comprise most of the swamp vegetation. The current regional humid tropical climate is marked by two dry and two wet seasons of unequal length and intensities.

The rainfall regime amounts to an average of  $1742 \pm 124$  mm/year between 1995 and 2015. The NSEW is drained by the Mengong stream, whose annual average discharge

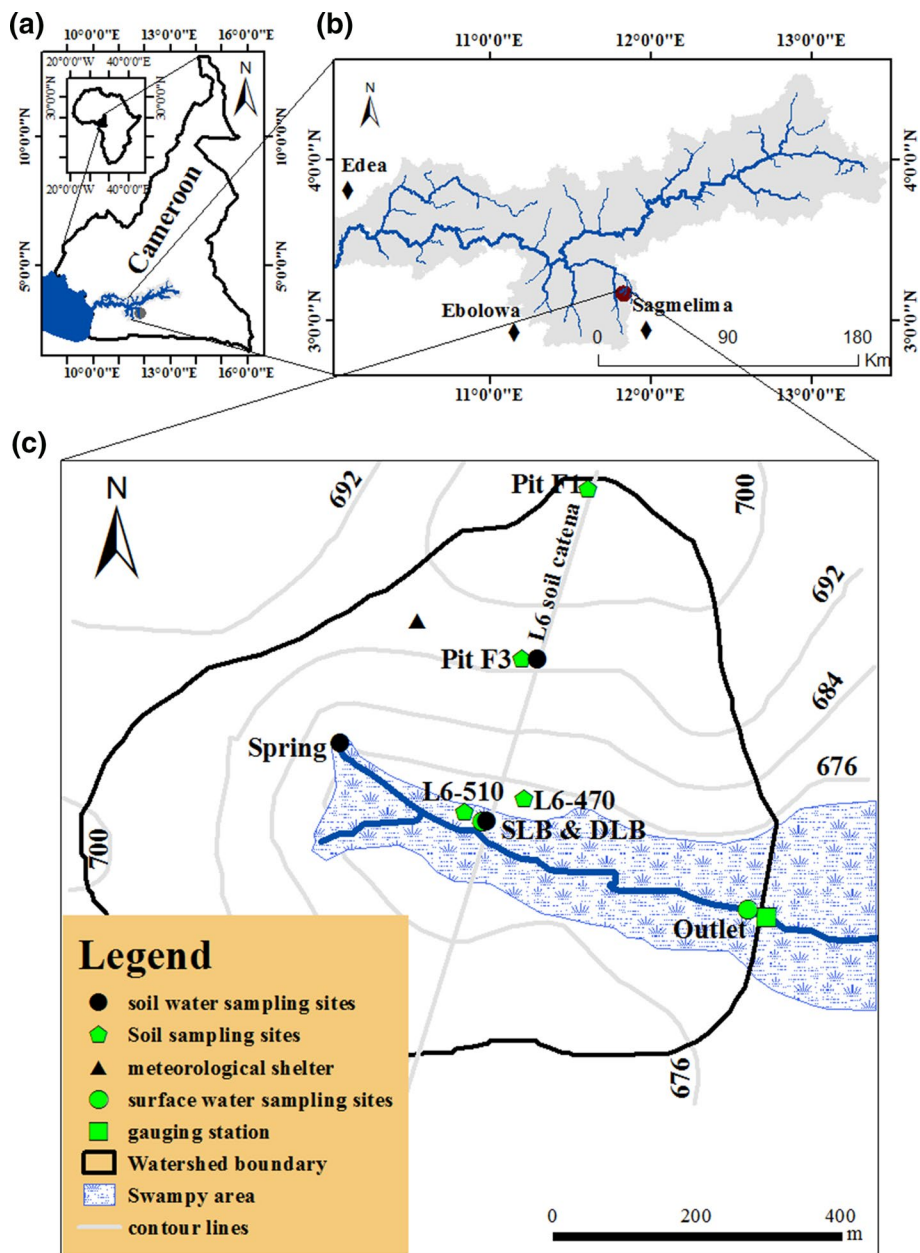


**Fig. 1** a Location of the Nyong river basin in the southern Cameroon and b location of the Nsimi Small Experimental Watershed (SEW) in the Nyong river basin and c map of the Nsimi SEW showing the swampy area (shaded area), the L6 soil catena, the spring, the outlet and the sampling sites alongside the main L6 catena

during the period 1995–2015 was  $7.8 \pm 5$  L/s at the outlet. The hydrological functioning of the catchment is governed by two main systems depending on water-table fluctuations: (1) a hillslope, with deeper water table, associated with essentially vertical water pathways and (2) a wetland where the water table usually reaches the soil surface during the wet season. A part of the water from deeper hillside aquifer emerges at specific seepage points and springs and is conveyed to the stream. The stream is adjacent to the wetland domain whose extent is highly variable between 8 and 20% of the total surface area of the catchment depending on hydroclimatic conditions (Braun et al. 2005). Maréchal et al. (2011) established the hydrological model for the catchment highlighting that the main contribution to streamflow is through the hillside aquifer which represents 64% of total stream flow. The second contribution of about 25% is from swamp overland flow during storm events. The groundwater flow from the swamp aquifer contributes to about 11% of streamflow.

### 3 Methods

The locations of the watershed sampling and the recording equipment have been described in Braun et al. (2005). A schematic cross section was generated along the L6 catena, in which some weathering profiles of the north hillside and of the swamp were selected for soil and groundwater sampling, as shown in Fig. 1.

#### 3.1 Soil/Litter Sampling and Preparation

Bulk soil samples of 1 kg were collected in each sampling point from the surface toward depth, in four open pits (F1, F3, L6-470 and L6-510) along the northern slope of the L6 catena (Fig. 1). Pit F1 was at the top of hill and pit F3 at the middle of hill. Pit L6-470 was at the hill–swamp transition, while pit L6-510 was in the saturated swampy area. Samples of the lateritic soil were collected in the soft clay topsoil horizon, within the first 2 m depth at pit F1 and 1 m depth at pit F3. In the hydromorphic soil, sampling was done in the organic-rich horizon, the clayey organic horizon and the sandy organic horizon within 1.5 m depth at pits L6-470 and 1 m depth at pit L6-510. The sampling depth was adapted to the thickness of the soil horizons, responding to the observed decrease in soil cover from the top of the hill toward the flat swamp. Considering that the horizon is constituted of layers with different material and different color, two to three samples were collected in each layer, depending on its thickness. After manual removal of large roots and gravels, soil samples were oven-dried at 45 °C for 5 days, separated with a sample divider, thoroughly homogenized and ground to fine powder. Bulk litter was collected at the vicinity of every soil sampling point, rinsed with distilled water, oven-dried at 45 °C for five days and then ground to fine powder.

#### 3.2 Water and TSS Sampling

Groundwater samples were collected monthly for a year from the hillside through piezometer installed at the bottom of the pit F3 at 8.5 m depth. Samples of wetland from the swamp aquifer were also collected monthly using two soil solution collectors implanted at depths of 0.4 m (surface low bottom—SLB) and 1.6 m (deep low bottom—DLB). The spring water was also sampled monthly, and discharge was measured continuously using a OTT water level recorder. These water samples were assumed to represent the main contributors



to streamflow in the catchment. Water from pit F3 and the springs represented the hillside aquifer, and that of DLB and SLB, respectively, represented the swamp aquifer and the saturated soil water of overland flows. Stream water was sampled fortnightly for a year at the outlet and discharge measured continuously using an OTT Thalimedes data logger. pH (pH 330i/SET probe, manufactured by WTW), temperature and conductivity (LF 325-B/SET probe, manufactured by WTW) were measured in the field.

Water samples were filtered in the field through 0.7- $\mu\text{m}$  filters (glass-fiber filters Whatman GF/F). The filters and the filtration unit were pre-rinsed with distilled water and then with a few mL of the sampled water. A 60-mL opaque glass vial was used for determining the concentration of DOC. Samples for stable carbon isotope analyses of DOC ( $\delta^{13}\text{C}_{\text{DOC}}$ ) were collected in 40-mL Trace Clean EPA vials, and samples for stable carbon isotope analyses of DIC ( $\delta^{13}\text{C}_{\text{DIC}}$ ) were collected in 500-mL glass bottles. Sealed high-density polyethylene bottles of 125 mL of raw water were collected for alkalinity titration. All the samples were treated with  $\text{HgCl}_2$  to prevent microbial activity. TSS was determined by filtering 500 mL of stream water through 0.7- $\mu\text{m}$  pre-combusted glass-fiber filters (Whatman GF/F). Filters were weighed before use, and after filtration, they were oven-dried at 60 °C during 6 h and then re-weighed. The TSS ( $\text{mg L}^{-1}$ ) is given as the difference between the two weights. POC and stable carbon isotope of POC ( $\delta^{13}\text{C}_{\text{POC}}$ ) were analyzed on total suspended sediment.

### 3.3 Soil and Water Analysis

The dry mass of total organic carbon (TOC), particulate organic carbon (POC) and total nitrogen (TN) was analyzed by combustion using a Carlo Erba analyzer (EA-CE 1500 NA), coupled with a Micromass Isochrom (EA-MS) continuous flow mass spectrometry for  $\delta^{13}\text{C}_{\text{TOC}}$ ,  $\delta^{13}\text{C}_{\text{POC}}$  and  $\delta^{15}\text{N}_{\text{TN}}$  determination at “Centro de Energia Nuclear na Agricultura Piracicaba Brazil. Soil, litter and TSS samples were prepared as follows. About 10 g of grounded or sieved sample was acidified by adding a solution of 1 N HCl, with a soil/solution ratio of 1:10. After agitation for 1 h, sample were rinsed with distilled water, then dried at 60 °C for 24 h and finally crushed. Thin capsules were used for sample loading in the elemental analyzer.

The TOC content was expressed as % of dry mass of ground sample. The average content of each layer was considered as the mean of its corresponding samples in the sampled pits. The  $\delta^{13}\text{C}$  and  $\delta^{15}\text{N}$  values are reported in the conventional delta notation as per mil deviation between the measured  $^{13}\text{C}/^{12}\text{C}$  and  $^{15}\text{N}/^{14}\text{N}$  ratios and the  $^{13}\text{C}/^{12}\text{C}$  and  $^{15}\text{N}/^{14}\text{N}$  ratios of the international standard Vienna Pee Dee Belemnite (V-PDB) and air, respectively, as follows (Craig 1957; Nier 1950):

$$\delta^{13}\text{C}(\text{‰}) = \left[ \left( \frac{(^{13}\text{C}/^{12}\text{C})_{\text{sample}}}{(^{13}\text{C}/^{12}\text{C})_{\text{standard}}} \right) - 1 \right] * 1000 \text{ and} \quad (1)$$

$$\delta^{15}\text{N}(\text{‰}) = \left[ \left( \frac{(^{15}\text{N}/^{14}\text{N})_{\text{sample}}}{(^{15}\text{N}/^{14}\text{N})_{\text{standard}}} \right) - 1 \right] * 1000. \quad (2)$$

Each sample was analyzed in duplicate, and the accuracy was  $\pm 0.2\text{‰}$  for  $\delta^{13}\text{C}$  and  $\pm 0.001\text{‰}$  for  $\delta^{15}\text{N}$ .

The Alkalinity titration using the Metrohm 716 DMS titrator was done within 24 h of sampling by Gran method with a 0.02 M HCl solution. The partial pressure  $\text{pCO}_2$  and the inorganic carbon species ( $\text{H}_2\text{CO}_3$ ,  $\text{HCO}_3^-$  and  $\text{CO}_3^{2-}$ ) were calculated from field pH



and alkalinity following Weiss (1974) after correction for temperature. DIC concentrations were derived by adding the inorganic carbon species. The accuracy of this calculation strongly depends on the quality of the pH measurements, for which field pH was used, the measurement having uncertainties of  $\pm 0.04$  pH units. Thus,  $p\text{CO}_2$  and DIC values calculated here characterize upstream catchments in non-carbonate environments, with low ionic strengths and low pH values, having errors of approximately  $\pm 11\%$  according to Marx et al. (2017).

DOC concentrations were determined using Pt-catalyzed, high-temperature combustion (680 °C) followed by infrared detection of  $\text{CO}_2$  using a Shimadzu TOC-5000 at Geosciences Lab, Toulouse, and  $\delta^{13}\text{C}_{\text{DOC}}$  was analyzed using a Finningan MAT DeltaPlus isotope ratio mass spectrometer at the G.G. Hatch Isotope Lab, Ottawa. Before DOC and  $\delta^{13}\text{C}_{\text{DOC}}$  analysis, filtered water samples were acidified by adding 1 mL of 1 N HCl to remove all traces of inorganic carbon, and then finally frozen and freeze-dried. For  $\delta^{13}\text{C}_{\text{DIC}}$  analysis, 20 mL of water sample was injected into 200-mL septum-sealed pre-combusted glass vials connected to a vacuum line. The glass vials were prefilled with 2 mL of concentrated phosphoric acid (85%) in order to convert all DIC species to  $\text{CO}_{2(\text{g})}$ . According to the procedure outlined by Kroopnick et al. (1970), the evolved  $\text{CO}_2$  was successively purified with a precision of 0.3‰ with liquid nitrogen and transferred into a glass tube by cryogenic trapping. The so-extracted  $\text{CO}_{2(\text{g})}$  samples were analyzed for  $\delta^{13}\text{C}$  composition using a VG OPTIMA mass spectrometer at the “Centre de Géochimie de la Surface” Lab, Strasbourg. The  $\delta^{13}\text{C}_{\text{DOC}}$  and  $\delta^{13}\text{C}_{\text{DIC}}$  are reported in the conventional delta notation as per mil with a precision of  $\pm 0.2\%$  (Eq. 1).

### 3.4 Determination of DIC Sources

The Keeling and Miller-Tans plot analyses were used to test the influence of soil-respired  $\text{CO}_2$  and DOC mineralization to the source of stream water DIC (Keeling 1958; Miller and Tans 2003). These approaches are particularly suitable for approximating the integrated  $\delta^{13}\text{C}$  of the DIC source when including multiple observations scattered in time or space. These models assume linearity, with simple mixing of carbon sources without further fractionation processes. Violation of these assumptions can occur as a result of nonlinear fractionation processes, such as kinetic fractionations (e.g.,  $\text{CO}_2$  evasion), Rayleigh distillation processes (e.g., photosynthesis) or biodegradation and photodegradation of DOC. This method is based on the mixing of isotopically distinct carbon sources and the combination of the principle of conservation of mass, presented as follows:

$$\delta^{13}\text{C}_{\text{obs}} * C_{\text{obs}} = \delta^{13}\text{C}_{\text{S}} * C_{\text{S}} + \delta^{13}\text{C}_{\text{B}} * C_{\text{B}} \quad (3)$$

where  $\delta^{13}\text{C}_{\text{obs}}$  and  $C_{\text{obs}}$  are the observed carbon isotopic composition and concentration, respectively, in each sample, resulting from a mixture of the carbon isotopic composition and concentration of the source. The suffix “S” represents the DIC source ( $\delta^{13}\text{C}_{\text{S}} \times C_{\text{S}}$ ) and suffix “B” ( $\delta^{13}\text{C}_{\text{B}} \times C_{\text{B}}$ ), atmospheric  $\text{CO}_2$ .

The Keeling and Miller-Tans regression plots (Eqs. 4 and 5, respectively) can be derived from Eq. (3) as the linear form ( $y = ax + b$ ):

$$\delta^{13}\text{C}_{\text{obs}} = C_{\text{B}} (\delta^{13}\text{C}_{\text{B}} - \delta^{13}\text{C}_{\text{S}}) * \left( \frac{1}{C_{\text{obs}}} \right) + \delta^{13}\text{C}_{\text{S}} \quad (4)$$

$$\delta^{13}\text{C}_{\text{obs}} * C_{\text{obs}} = \delta^{13}\text{C}_S * C_{\text{obs}} - C_B (\delta^{13}\text{C}_B - \delta^{13}\text{C}_S) \quad (5)$$

In stream water and groundwater with poor buffering capacity,  $\text{CO}_2$  evasion can shift the  $\delta^{13}\text{C}_{\text{DIC}}$  value by 1–4‰. Consequently, the interpretation of the  $\delta^{13}\text{C}_S$  derived from these mixing equations must be made with caution.

## 4 Results

### 4.1 Seasonal Variations of Rainfall, Stream Discharge and Water-Table Levels

Precipitation from rainfall occurred frequently throughout the year (Fig. 2a). There was no significant rainfall from mid-July to late August during the short dry season (SDS) and from late January to mid-February during the long dry season (LDS). Between early September and late October during the long rainy season (LRS), 54% of the total amount of

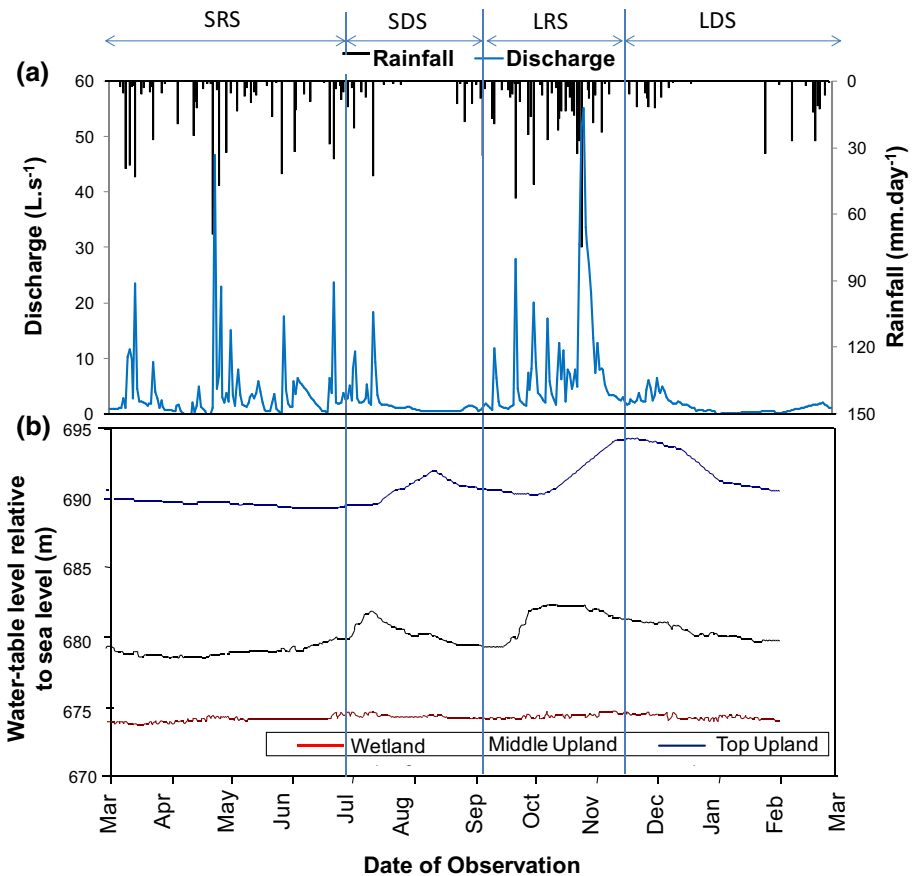


**Fig. 2** **a** Rainfall (bars) and stream discharge (solid line) showing the instantaneous hydrological reaction of the watershed (high discharge is correlated with high rainfall) and **b** water-table levels during the studied period

rainfall was observed. From mid-March to mid-July during the short rainy season (SRS), 46% of total rainfall was recorded. High amounts of rainfall (greater than 30 mm/day) were recorded during the months of March, May, June and July (Fig. 2a). It should be noted that the hydrological year considered in this study has been particular, characterized by a rainy season that extended until January, with an early return of precipitation as early as mid-February. This atypical hydrological profile has resulted in maintaining near-permanent wetness in the watershed throughout the hydrological cycle. Stream discharge from the Mengong was generally in sync with the rainfall. High discharge rates greater than 30 L/s corresponded to high rainfall events in early May and late October.

Fluctuations in water levels were low but in sync with seasonal variations of rainfall in the swamp. (Fig. 2b). The swamp was mostly saturated during the rainy seasons overflowing into the stream. These fluctuations were more pronounced in hillslope, with a delay of the peaks compared to that of precipitation, thus reflecting a 1-month average recharge period. Water levels dropped during the dry seasons, with lowest water levels observed during the LDS on the hilltop, while remaining below ground level in the swamp location.

#### 4.2 TOC and TN Contents and $\delta^{13}\text{C}_{\text{TOC}}$ and $\delta^{15}\text{N}_{\text{TN}}$ Composition in Soil Profiles

The TOC and TN concentrations and  $\delta^{13}\text{C}_{\text{TOC}}$  and  $\delta^{15}\text{N}_{\text{TN}}$  values are summarized in Table 1.

TOC in ferrallitic soil from F1 and F3 (Fig. 3a) decreased with depth. In the thin humus layer (5–10 cm), the average TOC was  $7.0 \pm 1.0$  wt % and decreased sharply in the clayey overlay to an average of 0.5 wt % at 100 cm. The hydromorphic soil (Fig. 3c) had higher TOC contents of 14.4 wt % on average in the first 0–10 cm of the organic-rich layer. The TOC remained higher at L6-510 and decreased steadily in the clayey organic layer and the sandy organic layer where TOC content was up to 3.0 wt % at 70 cm depth. At L6-470, TOC decreased sharply to 0.8–35 cm depth. The TOC content in litter ranged between 24.9 and 26.0 wt % under forest. Litter under fallow vegetation had TOC content of 16.7 wt %, and that under aquatic grass at the shallow swamps was 22.5 wt %. The profiles of the hillside ferrallitic soils had no measurable TN. Nitrogen contents in hydromorphic soils of the shallow swamps at L6-510 were relatively low between 1.3 wt % at 5 cm in the organic-rich layer and 0.1 wt % at 70 cm in the clayey and sandy organic layer. TN in litters ranged between 0.7 and 2.4 wt %.

In the ferrallitic soil profiles,  $\delta^{13}\text{C}_{\text{TOC}}$  varied between  $-19.8\text{‰}$  and  $-30.8\text{‰}$  (Fig. 3b). Surface litter sampled around F1 and F3 was more enriched with  $\delta^{13}\text{C}_{\text{TOC}}$  values of  $-21.1\text{‰}$  and  $-19.8\text{‰}$ , respectively. Below the surface, the thin humus layer between 0 and 10 cm depth was most depleted with  $\delta^{13}\text{C}_{\text{TOC}}$  between  $-30.8$  and  $-28.4\text{‰}$ . Deeper in the clayey overlay,  $\delta^{13}\text{C}_{\text{TOC}}$  was enriched by up to 5‰ and then stabilizes to around  $-25 \pm 0.7\text{‰}$  on average. In hydromorphic soil profiles,  $\delta^{13}\text{C}_{\text{TOC}}$  varied between  $-17.9$  and  $-31.1\text{‰}$  (Fig. 3d). Surface litter from both L6-470 and L6-510 was relatively depleted with  $\delta^{13}\text{C}_{\text{TOC}}$  of  $-31\text{‰}$ . In the organic-rich layer, between 5 and 10 cm in L6-470, there was a further increase in  $\delta^{13}\text{C}_{\text{TOC}}$  to  $-20.5\text{‰}$ . In L6-510, the observed  $\delta^{13}\text{C}_{\text{TOC}}$  increase was more pronounced to  $-17.9\text{‰}$  and extended to the clayey and sandy layers at 50 cm depth. Between 10 and 150 cm and 70 and 100 cm in L6-510 and L6-470, respectively,  $\delta^{13}\text{C}_{\text{TOC}}$  decreased to values averaging  $-28 \pm 0.7 \text{‰}$ . Litter under forest and fallow at F1, F3 and L6-470 had TN content between 0.7 and 1.9% and  $\delta^{15}\text{N}_{\text{TN}}$  between 3.6 and 8.2‰. TN content was not measurable in these soil profiles. In hydromorphic soil of the shallow

**Table 1** Values and ranges of TOC, TN,  $\delta^{13}\text{C}$  and  $\delta^{15}\text{N}$  in litters and soil profiles and termite mounds of the Mengong catchment

Soil type	Position from sea level	Depth (cm)	% TOC	$\delta^{13}\text{C}_{\text{TOC}}$ (‰)	% TN	$\delta^{15}\text{N}_{\text{TN}}$ (‰)	Soil layer description
Ferrallitic soils of the hillside	Pit F1 (top hill) Altitude 710 m	0	26.0	-21.1	1.9	5.1	Litter under fallow
		0-10	7.7	-30.8	<DL	<DL	Thin humus layer
		10-40	1.1	-25.3	<DL	<DL	Organic clayey overlay
		40-75	0.8	-26.2	<DL	<DL	Gray clayey overlay
		75-100	0.7	-25.2	<DL	<DL	Brown clayey overlay
	Pit F3 (middle hill) Altitude 694 m	100-200	0.4	24.9	<DL	<DL	
		0	16.7	-19.8	1.1	5.1	Litter under fallow
		0-5	6.3	-26.6	<DL	<DL	Thin humus layer
		5-10	1.5	-26.6	<DL	<DL	Organic clayey overlay
		10-25	0.8	-25.9	<DL	<DL	Gray clayey overlay
	25-60	0.8	-25.4	<DL	<DL	Brown clayey overlay	
	60-90	0.9	-26.5	<DL	<DL		
	90-100	0.5	-25.4	<DL	<DL		

**Table 1** (continued)

Soil type	Position from sea level	Depth (cm)	% TOC	$\delta^{13}\text{C}_{\text{TOC}}$ (‰)	% TN	$\delta^{15}\text{N}_{\text{TN}}$ (‰)	Soil layer description	
Hydromorphic soils of the swampy area	Profile L6-470 (hill/swamp transition) Altitude 674 m	0	24.9	-31.0	0.7	8.0	Litter under swamp forest	
		0-10	14.6	-20.5	<DL	<DL	Organic-rich layer	
		10-35	0.8	-28.9	<DL	<DL	Clayey organic layer	
		35-55	0.6	-28.5	<DL	<DL	Dark sandy layer	
		55-80	0.3	-27.9	<DL	<DL	Gray sandy layer	
		80-100	0.2	-26.9	<DL	<DL		
		100-120	0.4	-28.8	<DL	<DL		
		120-150	0.3	-28.6	<DL	<DL		
		0	22.5	-31.1	2.4	3.6	Litter under raffia palms and aquatic grass	
		0-5	16.2	-26.2	1.3	6.3	Organic-rich layer	
Termite mounds	Profile L6-510 (low marshes) Altitude 672 m	0-10	12.4	-20	1.1	8.2		
		10-20	9.1	-18.9	0.4	6.5	Clayey organic layer	
		20-40	10.49	-17.9	0.5	6.8	Clayey and sandy organic layer	
		40-50	5.13	-21.2	0.2	7.1	Gray sandy layer	
		50-70	3.06	-25.3	0.1	5.4		
		70-100	0.07	-28.4	<DL	<DL		
		T1	2.3	-27.3	1.4	5.6	"Pagoda" termite mound	
		T2	2.5	-26.7	1.2	5.7	"Topless" termite mound	

<DL below the detection limit

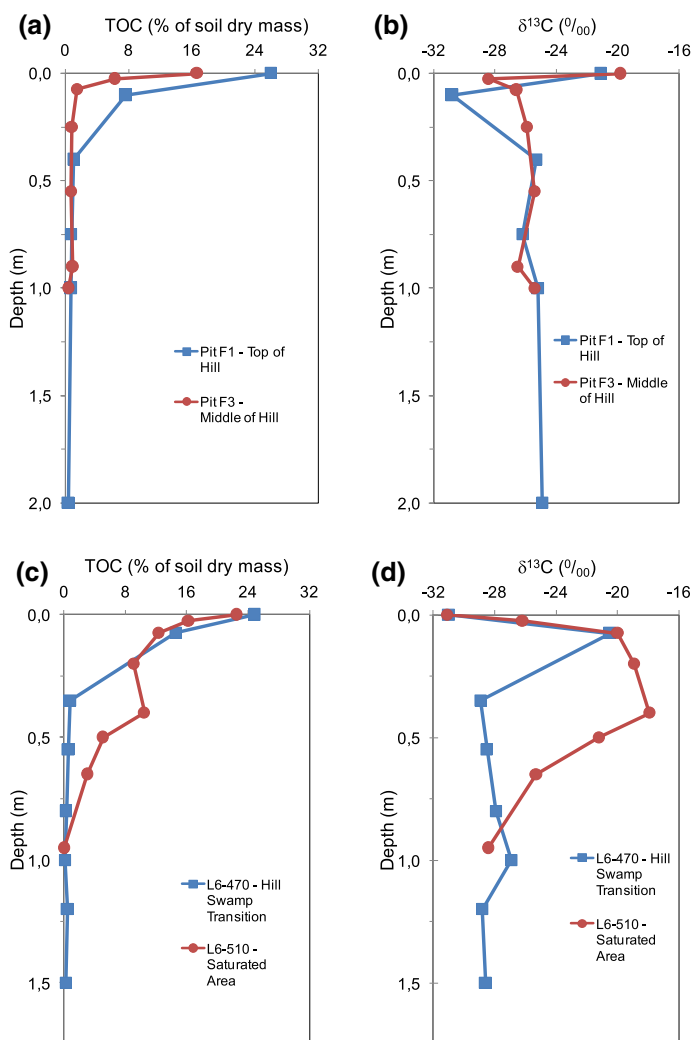


**Fig. 3** Variation of total organic carbon content (TOC) and the values of TOC stable carbon isotope ( $\delta^{13}\text{C}_{\text{TOC}}$ ) with soil depth (m) for the hillside soils (a, b) and for the wetland soils (c, d)

swamps (pit L6-510), TN content in litter was 2.4% and declined with depth from 1.3% in the organic-rich layer at 10 cm depth to 0.1% in the clayey and sandy layer at 70 cm depth.

### 4.3 DOC and POC Concentrations, and $\delta^{13}\text{C}_{\text{DOC}}$ and $\delta^{13}\text{C}_{\text{POC}}$ Compositions in Soil and Stream Water

DOC and POC concentrations, and  $\delta^{13}\text{C}_{\text{DOC}}$  and  $\delta^{13}\text{C}_{\text{POC}}$  in water sampled from hillside groundwaters (pit F3 and spring), groundwater of swamps (DLB), saturated soil water of swamps (SLB) and stream water are presented in Table 2. DOC concentrations in all groundwaters were low and varied between 0.3 and 4.5 mg/L, showing just a slight positive

**Table 2** Ranges (maximum, minimum, mean and standard deviation) of temperature ( $T^{\circ}\text{C}$ ), pH, alkalinity, log partial pressure of carbon dioxide (log  $\text{pCO}_2$ ), DOC and DIC content,  $\delta^{13}\text{C}_{\text{DIC}}$  and  $\delta^{13}\text{C}_{\text{DOC}}$  isotopic signatures in soil water (SLB), groundwater (Pit F3 and DLB), spring water and stream water of the NSEW

Sampling site	$T^{\circ}\text{C}$	Field pH	Alk ( $\mu\text{eq/L}$ )	log $\text{pCO}_2$	DIC (mg/L)	$\delta^{13}\text{C}_{\text{DIC}}$ (‰)	DOC (mg/L)	$\delta^{13}\text{C}_{\text{DOC}}$ (‰)	POC (mg/L)	$\delta^{13}\text{C}_{\text{POC}}$ (‰)
<i>Spring</i>										
Max	26.7	6.6	78.5	-2.0	25.6	-7.4	1.2	-26.3	na	na
Min	22.7	4.7	55.9	-3.0	1.3	-20.9	0.3	-28.6	na	na
Mean	23.6	5.1	66.4	-2.5	16.9	-14.2	0.4	-27.0	na	na
SD	1.2	0.6	6.8	0.4	8.4	5.0	0.2	0.6	na	na
<i>Pit F3</i>										
Max	25.9	6.1	81.5	-2.1	29.2	-9.1	4.5	na	na	na
Min	22.6	4.5	35.8	-3.0	2.8	-20.4	0.4	na	na	na
Mean	23.5	5.0	50.3	-2.5	10.6	-14.5	1.4	na	na	na
SD	1.0	0.5	15.0	0.3	7.6	4.4	1.2	na	na	na
<i>DLB</i>										
Max	26.3	6.8	168.9	-2.0	40.8	-6.6	3.0	na	na	na
Min	22.4	4.9	134.0	-2.9	2.3	-20.2	0.5	na	na	na
Mean	23.7	5.6	155.7	-2.5	20.1	-12.5	0.9	na	na	na
SD	1.1	0.6	13.6	0.3	12.3	5.5	0.7	na	na	na
<i>SLB</i>										
Max	26.3	6.6	216.0	-2.1	39.2	-8.8	18.2	na	na	na
Min	21.9	4.9	50.7	-2.9	1.8	-22.2	1.7	na	na	na
Mean	24.2	5.5	122.6	-2.5	17.2	-16.3	8.0	na	na	na
SD	1.4	0.6	47.3	0.3	10.7	4.0	5.9	na	na	na
<i>Stream</i>										
Max	28.8	6.2	140.8	-1.5	15.7	-14.2	29.6	-29.0	4.8	-28.0
Min	21.2	5.1	25.6	-2.7	1.0	-23.0	12.7	-29.5	0.1	-29.9
Mean	23.9	5.5	81.0	-2.0	6.1	-20.0	21.7	-29.3	1.8	-29.0
SD	1.7	0.3	31.3	0.3	3.2	2.4	4.5	0.2	1.2	0.7

na not analyzed



shift at the beginning of the SRS (Fig. 4b). In SLB and stream water, DOC concentration varied between 1.7 and 18.2 mg/L and 14.6 and 30.5 mg/L, respectively, with peaks observed most often during rainy seasons (SRS and LRS). POC was low in the stream samples (Table 2), with concentration ranging between 0.1 and 4.8 mg/L, representing on average  $24.8 \pm 5.4\%$  of total suspended sediment (TSS). The stream POC variation was in sync with TSS, increasing slightly at the beginning of the rainy seasons (Fig. 4c). The notable peak of POC was observed during the LDS.

$\delta^{13}\text{C}_{\text{DOC}}$  in stream water of the Mengong brook was  $-29.3 \pm 0.2\text{‰}$ , generally 2.3‰ units lighter than that of the spring ( $-27.0 \pm 0.6\text{‰}$  on average, Table 2). Little temporal variation of the  $\delta^{13}\text{C}_{\text{DOC}}$  was observed for the spring with more depleted values observed during LRS and heavier values during LDS. Slight shift was observed for  $\delta^{13}\text{C}_{\text{POC}}$  that fluctuated between  $-29.9$  and  $-28.0\text{‰}$  during the sampling period, with increases observed at the beginning of the rainy periods.

#### 4.4 $T$ , pH, $\text{pCO}_2$ , DIC Concentrations and Stable Carbon Isotope Composition ( $\delta^{13}\text{C}_{\text{DIC}}$ )

Temperature ranged from 22.3 to 26.7 °C, averaging  $23.8 \pm 1.4$  °C. In general, temperature decreased between March and August and increased slightly between September and February. All the pH of the samples was acidic, ranging between 4.5 and 6.8, the lowest pH values being observed for hillside groundwaters (pit F3 and spring). Generally, pH was less acidic at the beginning of the SRS. Alkalinity ranged from 25.6 to 216.0  $\mu\text{eq/L}$ , and samples from SLB and DLB were more alkaline than those of hillside groundwaters (pit F3 and spring). All samples were saturated in  $\text{CO}_2$ , with log  $\text{pCO}_2$  ranging from  $-2.98$  to  $-1.46$  atm and averaging  $-2.3 \pm 0.4$  atm (Table 2). Higher values of  $\text{pCO}_2$  were observed for stream water.  $\text{pCO}_2$  was low during the SRS and the SDS and high during the LRS and the LDS.

The DIC concentrations from the SLB, DLB and the spring were comparable ( $17.2 \pm 10.7$  mg/L;  $20.1 \pm 12.3$  mg/L;  $16.9 \pm 8.4$  mg/L on average, respectively) but higher than that in samples from the pit F3 ( $10.6 \pm 7.6$  mg/L on average). Stream DIC concentrations were relatively low ( $6.1 \pm 3.2$  mg/L on average), compared to that of groundwater samples. DIC concentrations dropped during the rainy seasons and increased during the dry season, with lowest DIC values recorded during the SRS (Fig. 5b). This pattern is observed for both stream and groundwater.

$\delta^{13}\text{C}_{\text{DIC}}$  isotopic compositions were similar in groundwaters (spring, F3 and DLB), varying between  $-20.9$  and  $-6.6\text{‰}$  and generally enriched with regard to saturated soil water of swamps (SLB between  $-22.2$  and  $-8.8\text{‰}$ ) (Table 2). The  $\delta^{13}\text{C}_{\text{DIC}}$  of stream water samples was more depleted than those of groundwaters and soil water, varying between  $-14.2$  and  $-23.0\text{‰}$ . In general,  $\delta^{13}\text{C}_{\text{DIC}}$  exhibited similar patterns in all the sampling locations. The  $\delta^{13}\text{C}_{\text{DIC}}$  of groundwaters and soil water was enriched during the SRS and SDS and was depleted during the LRS and LDS (Fig. 5c). The seasonal shift of stream water  $\delta^{13}\text{C}_{\text{DIC}}$  was comparable to that of samples from SLB. A general decrease in  $\delta^{13}\text{C}_{\text{DIC}}$  was observed at the beginning of the SRS. This depletion was more pronounced during the LRS reaching the most depleted values at the end of the LDS (Fig. 5c).

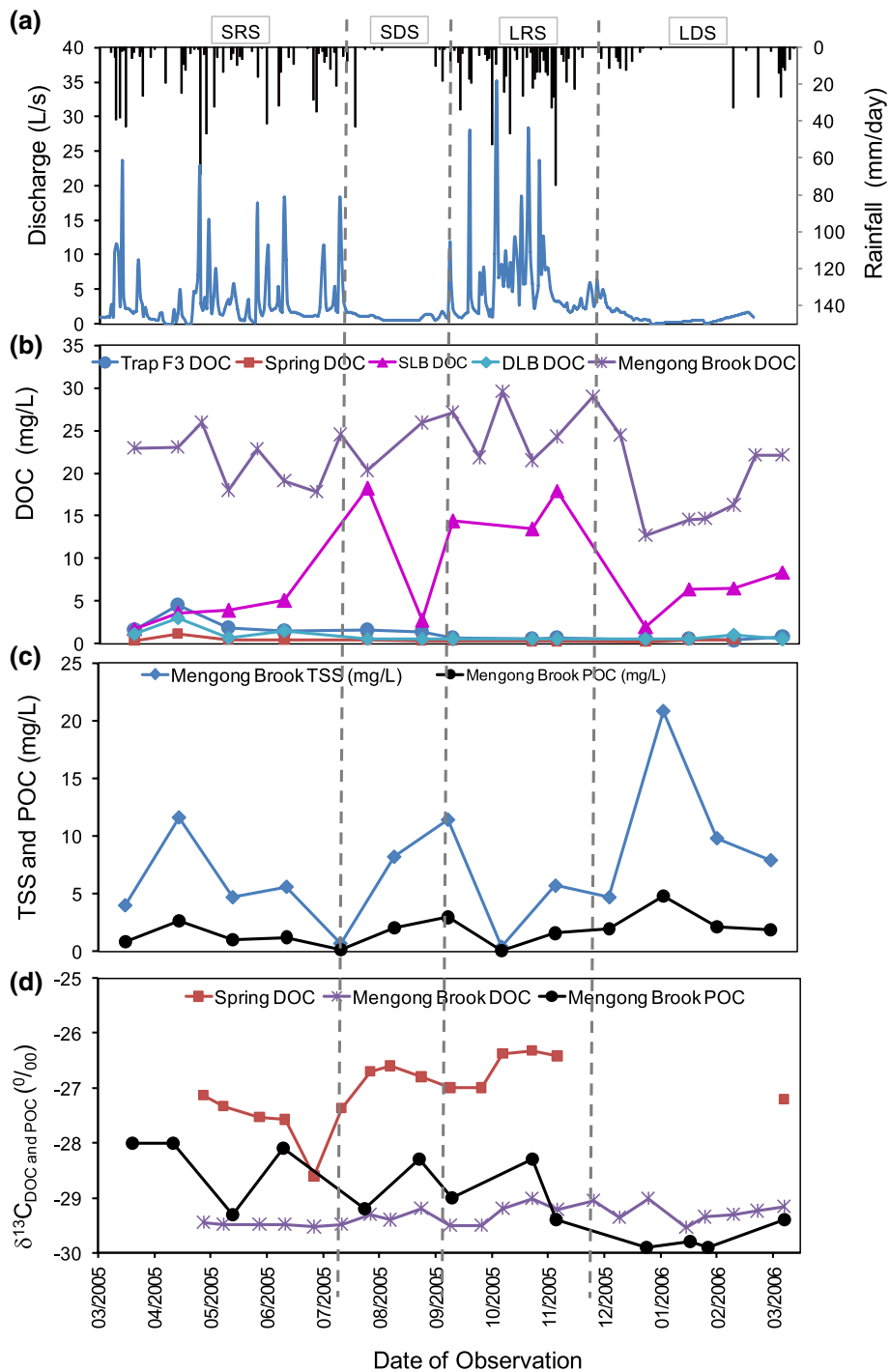
**Fig. 4** **a** Seasonal variation of rainfall and discharge plotted with **b** the seasonal shift of DOC, **c** TSS and **d** POC concentrations in stream water and **d** the seasonal shift of  $\delta^{13}\text{C}_{\text{DOC}}$  and  $\delta^{13}\text{C}_{\text{POC}}$  values in spring water and stream water. The shaded lines represent the separations of the four major seasons (*SRS* small rainy season, *SDR* small dry season, *LRS* long rainy season, *LDS* long dry season)

## 5 Discussion

This section explains the surface water, groundwater and stream water  $\delta^{13}\text{C}$  of DOC, DIC and POC values, highlighting the sharp linkage between soil organic carbon and stream DOC, demonstrating that DIC transformations are regulated by different biogeochemical processes other than atmospheric  $\text{CO}_2$  evasion. We also highlight the main processes that control carbon transformation in soils and stream of this headwater catchment. The dependence of carbon sources to the seasonal water changes and the relationship with different carbon pools to the stream are also discussed.

### 5.1 Linkage Between Soil Organic Carbon and Stream DOC, POC and DIC

The distribution of TOC and  $\delta^{13}\text{C}_{\text{TOC}}$  in the NSEW displayed a vertical and lateral variation along the slope between the hillside and the swamp wetland. These variations are ideal in linking soil organic material sources to stream DOC and POC and for detecting potential temporal changes in stream DOC and POC sources (Balesdent and Mariotti 1996; Amiotte-Suchet et al. 1999; Lambert et al. 2011). TOC content decreases sharply with depth in hillside ferrallitic soil, suggesting a high rate of organic carbon turnover with depth and leading to soil-derived carbon dioxide ( $\text{CO}_2$ ) and DIC. In contrast, the accumulation of rich TOC content in saturated soil water of swamps might justify the high DOC concentration observed in both the soil water of the swamps and stream water, and the poor DIC delivery to the stream. Earlier studies in this catchment show that two types of water can be distinguished depending on DOC and DIC concentrations: (1) clear water (spring water, deep groundwater from pit F3 and DLB) with low DOC concentration and significantly high DIC concentration, representing about 20% of the stream flow and (2) dark tea water (saturated soil waters from wetland and stream water) with high DOC concentration and relatively low DIC concentration (especially for the stream water) (Ndam Ngoupayou et al. 2005b; Viers et al. 1997; Olivia et al. 1999; Boeglin et al. 2005; Brunet et al. 2009). This notable difference of DOC and DIC contents between groundwater of deeper horizon and saturated soil water of wetland and stream has equally been observed in several catchments (Amiotte-Suchet et al. 2007; Sanderman et al. 2009; Lambert et al. 2011; Huang et al. 2013; Campeau et al. 2018). This suggests that processes that convert initial organic material to DOC and DIC are different in both the hillside and wetland soils. Although the DIC content was a bit higher in the springs with respect to the stream outlet which justifies carbon evasion in the transfer process in both studies. We observe, however, that  $\delta^{13}\text{C}_{\text{DIC}}$  for our study was more depleted at the outlet of the river with regard to the spring, which is contrary to what was observed by Brunet et al. (2009). The hydrological model of this catchment (Ndam Ngoupayou et al. 2005a, b; Braun et al. 2005; Maréchal et al. 2011) shows that spring water originates from hillside aquifers. This justifies the comparable enriched  $\delta^{13}\text{C}_{\text{DIC}}$  from hillside aquifer and spring water. Our depleted  $\delta^{13}\text{C}_{\text{DIC}}$  observed in spring water could be related to water supplied from swampy areas which has more depleted  $\delta^{13}\text{C}_{\text{DIC}}$  with high DOC concentrations. As a consequence, carbon evasion cannot



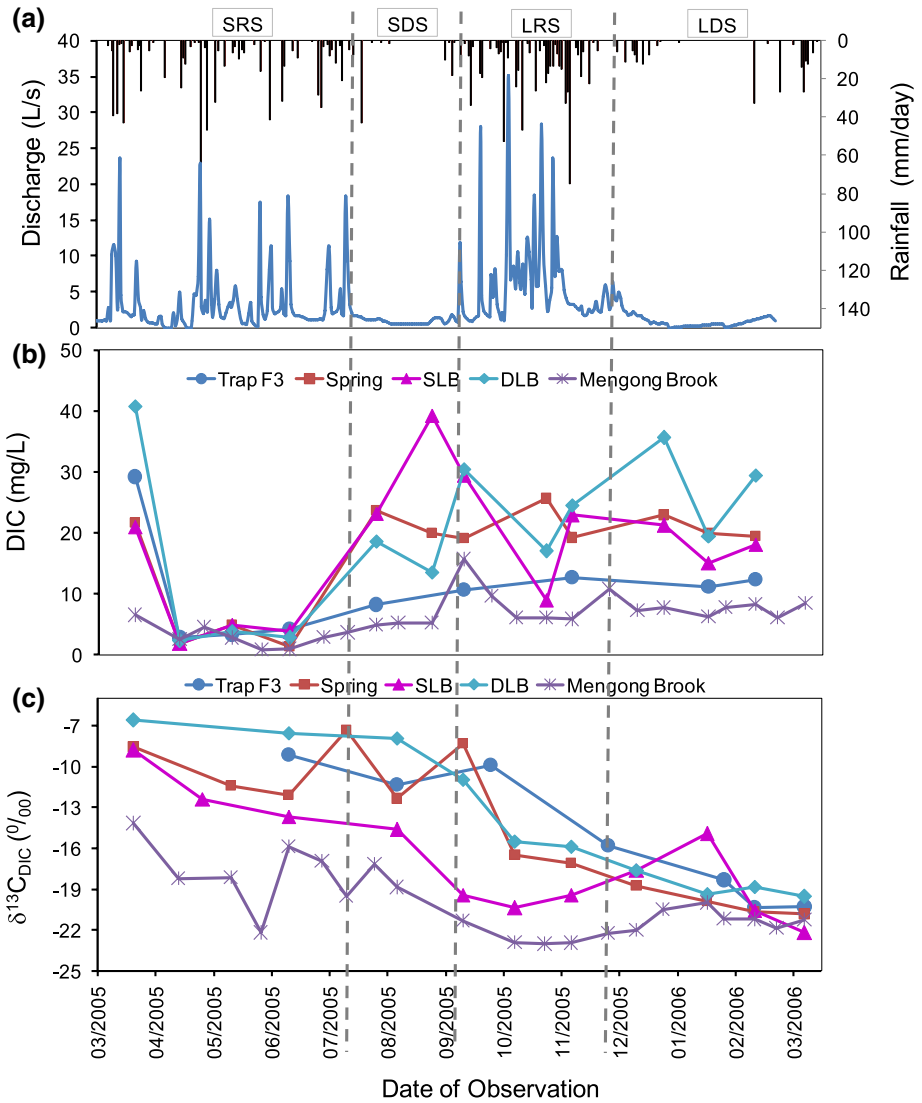


**Fig. 5** a Seasonal variation of discharge plotted with b the seasonal shift of DIC concentrations and c the seasonal shift of  $\delta^{13}\text{C}_{\text{DIC}}$  values in soil waters and stream water. The shaded lines represent the separations of the four major seasons (SRS small rainy season, SDR small dry season, LRS long rainy season, LDS long dry season)

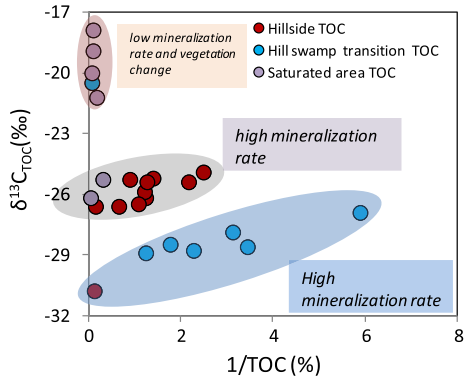
be used alone to justify the variation of isotopic composition between the spring and the stream outlet.

In the NSEW, the isotopic composition of SOM, the primary source of DOC and POC in the stream water, is typical of C3 plant cover, with  $\delta^{13}\text{C}$  of  $-30.8$  to  $-26.6\text{‰}$  for the thin humus layer in ferrallitic soil and an enrichment by  $1\text{--}6\text{‰}$  in  $\delta^{13}\text{C}$  values with increasing depth. These types of depth trends where TOC decreases while  $\delta^{13}\text{C}_{\text{TOC}}$  is enriched are common to a number of environments, with stable C3 ecosystem (Balesdent and Mariotti 1996; Koutika et al. 1997; Powers and Schlesinger 2002; Wynn and Bird 2007). Previous studies show that, in well-drained and undisturbed soil profiles, as observed on the hillside, decomposer organisms would prefer labile  $^{13}\text{C}$ -depleted molecules for respiration, while residual  $^{13}\text{C}$ -enriched molecules tend to be used in the production of biomass and the end-products of the metabolism (Ngao and Cotrufo 2011; Krüger et al. 2014). This observation is consistent with the positive relationship between  $\delta^{13}\text{C}_{\text{TOC}}$  versus  $1/\text{TOC}$  (Fig. 6) indicating a high rate of mineralization of SOM in accordance with the intense faunal activities observed in these hillslope soils (Diochon and Kellman 2008). This could lead to the observed enrichment of the  $\delta^{13}\text{C}_{\text{TOC}}$  of termite mounds with values of  $-27\text{‰}$  (Table 1) relative to the initial SOM components. The hydromorphic soil of the saturated area shows a clearly different pattern with no relationship observed for  $\delta^{13}\text{C}_{\text{TOC}}$  versus  $1/\text{TOC}$  (Fig. 6). As previously reported by Day et al. (1988), water retention in the swamp maintains a permanent soil saturation, limiting the activity of the soil aerobic microorganisms, leading to low mineralization rate of soil organic matter. This therefore promotes the accumulation of organic matter in this zone. In addition, the average isotopic enrichment of  $7\text{‰}$  units in the organic-rich horizon of hydromorphic soils cannot be entirely explained by the isotopic fractionation during the mineralization processes of SOM. This isotopic enrichment might also be due to mixing from plant materials supplied from  $^{13}\text{C}$ -enriched vegetation such as C3 plant and plant component from maize crop of C4 type (Wynn et al. 2006). This observation could be explained by the aquatic grassland of C4 type which has been developed in this shallow swampy area, coupled with maize crop cultivation. The current heavier  $\delta^{13}\text{C}_{\text{TOC}}$  of  $-19.8$  to  $-21.1\text{‰}$  observed for hillside litters could be a result of this.

$\delta^{13}\text{C}_{\text{TOC}}$  values of hillside soils were comparable (showing just a little shift of  $1\text{‰}$ ) with relatively enriched  $\delta^{13}\text{C}_{\text{DOC}}$  values of groundwater (springs). This result is consistent with several studies from small forested catchments, in which upland DOC was found to drop with increasing depth, with an accompanying increase in  $\delta^{13}\text{C}_{\text{DOC}}$  (Amiotte-Suchet et al. 2007; Sanderman et al. 2008, 2009; Huang et al. 2013). However,  $\delta^{13}\text{C}_{\text{TOC}}$  values of the swampy rich TOC soils were generally higher than  $\delta^{13}\text{C}_{\text{DOC}}$  values of rich DOC stream water, which calls for attention in the interpretation of DOC drivers in stream water. Regarding POC, the relatively constant  $\delta^{13}\text{C}_{\text{POC}}$  values observed in this catchment suggest a first-order conservative behavior that occurs during the delivery of SOC to stream (Gao et al. 2007). The predominance of a biogenic source is evident in the sampled waters with depleted  $\delta^{13}\text{C}_{\text{DIC}}$  accompanying a lower DIC concentration (Shin et al. 2011). As observed by Campeau et al. (2018), the low DIC and high  $\text{pCO}_2$  values observed in stream relative to adjacent groundwaters indicate that substantial gas losses to the atmosphere occurred during transport from soils to streams. Furthermore, despite the observed gas losses to the atmosphere, the  $\delta^{13}\text{C}_{\text{DIC}}$  values of stream water remain low compared to groundwater, demonstrating that DIC transformation in soils and stream is regulated by several different biogeochemical processes and not strictly by atmospheric  $\text{CO}_2$  evasion.

In this study area, the tropical hot and wet climate will favor the intense decomposition of native SOC which will lead to production of DOC; soil  $\text{CO}_2$  and residuals (from which POC derives). Increasing precipitation could lead to dilution of the resulting DOC in soil

**Fig. 6**  $\delta^{13}\text{C}_{\text{TOC}}$  versus  $1/\text{TOC}$  in soil profiles of hillside and swamps (the mineralization of SOM with depth caused the decrease in TOC and the increase in  $\delta^{13}\text{C}_{\text{TOC}}$  in hillside profiles. This pattern was not found in swampy soils where the shift of  $\delta^{13}\text{C}_{\text{TOC}}$  was due to the vegetation change between C3 and C4 plants)



water and to dissolution of gaseous  $\text{CO}_2$  to DIC, thereby increasing the DIC and lowering the DOC concentration of spring water (Huang et al. 2013). Additionally, the higher clay and silt content in the soft clayey topsoil horizon might lead to higher adsorption capacity of DOC in the soil, resulting in lower export of soil DOC (Nelson et al. 1993). Figure 7 represents the relationship of  $\delta^{13}\text{C}_{\text{DOC}}$  versus  $1/\text{DOC}$  and explains the trend of decreasing DOC with a corresponding increase in  $\delta^{13}\text{C}_{\text{DOC}}$ . According to Lambert et al. (2011), such relation may occur in cases where DOC is transported mostly laterally through microbial active soil horizons. Such transportation enhances the biodegradation of soil DOC associated with the removal of  $^{12}\text{C}$ , which could result in the increase in residual  $\delta^{13}\text{C}_{\text{DOC}}$  in spring water (Opsahl and Zepp 2001). However, the low soil DOC with heavier  $\delta^{13}\text{C}_{\text{DOC}}$  values from the hillside did not constrain the stream DOC, which remained higher with more depleted  $\delta^{13}\text{C}_{\text{DOC}}$ . The  $\delta^{13}\text{C}_{\text{DOC}}$  ( $-29.1$  to  $-29.5\%$ ) and  $\delta^{13}\text{C}_{\text{POC}}$  ( $-28.0$  to  $-29.9\%$ ) for stream water are consistent with  $\delta^{13}\text{C}$  values measured for TOC in the organic layer and the litters under swampy forest ( $-28.4$  to  $-31.0\%$ ). Both  $\delta^{13}\text{C}_{\text{DOC}}$  and  $\delta^{13}\text{C}_{\text{POC}}$  show no significant seasonal shift, because the main source of organic carbon in the stream is limited to the subsurface soils of the shallow swampy area. The absence of seasonal fluctuations in  $\delta^{13}\text{C}_{\text{DOC}}$  could explain a single process of stream DOC, almost exclusively limited in this case, to the leaching of the upper soil layers of the swamp. As concerns POC, in-stream remobilization of organic carbon from plant materials and the leaching of swamp would be important, since constant values of  $\delta^{13}\text{C}_{\text{POC}}$  could indicate a single dominant source.

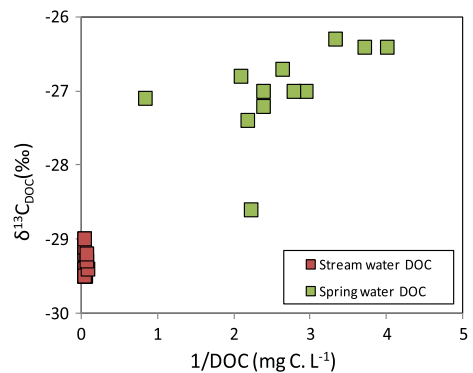
## 5.2 Identification of Drivers of $\delta^{13}\text{C}_{\text{DIC}}$

In freshwater catchment, the variability of DIC content and  $\delta^{13}\text{C}_{\text{DIC}}$  values depends on the large equilibrium fractionations that exist within the carbonate system (Zhang 1995; Zeebe and Wolf-Gladrow 2001) driven by pH and alkalinity. Acidic freshwaters where alkalinity and pH are low are almost related to small isotopic fractionations, because the influence of  $\text{CO}_2$  evasion on  $\delta^{13}\text{C}_{\text{DIC}}$  values remains low (Doctor et al. 2008; Venkiteswaran et al. 2014). In this study, the  $\delta^{13}\text{C}_{\text{DIC}}$  values observed in the stream water and groundwater of the NSEW were remarkably negative, reflecting the biogenic sources from mineralization of organic carbon. Despite the observed low alkalinity and pH for the water samples in the headwater catchments, we observed a larger variability in  $\delta^{13}\text{C}_{\text{DIC}}$  values (ranging from  $-6.6$  to  $-23.0\%$ ) far above the typical isotopic fractionations of  $<4\%$  expected for such

waters. This suggests several processes modulating the DIC (Mayorga et al. 2005; Hotchkiss et al. 2015; Campeau et al. 2017, 2018). In order to circumscribe the DIC source and to understand the drivers on  $\delta^{13}\text{C}_{\text{DIC}}$  values, we used the Keeling and Miller-Tans plots analysis which are suited to test the influence of soil-respired  $\text{CO}_2$  on DIC source. The results show no significant relationship in the Keeling plots ( $\delta^{13}\text{C}_{\text{DIC}}$  as a function of  $1/\text{DIC}$ ), either by combining all sampling points or individual points (Fig. 8a). Despite the lack of relationship in the Keeling plots, we observed a decrease in stream water DIC which come along with low  $\delta^{13}\text{C}_{\text{DIC}}$  values compared to groundwater. This suggests that the isotopic effect of  $\text{CO}_2$  evasion is mixed with additional processes. The Miller-Tans plots ( $\delta^{13}\text{C}_{\text{DIC}} \times \text{DIC}$  as a function of DIC concentration) revealed a highly significant linear relationship for the stream water  $\delta^{13}\text{C}_{\text{DIC}}$  values, but a poor linear relationship for groundwater (Fig. 8b). The  $\delta^{13}\text{C}_{\text{DIC}}$  source, approximated by the slope in the Miller-Tans plot, was  $-22.5\%$  for stream water and between  $-11.0$  and  $-17.0\%$  in groundwater, showing two major groups.

These discrepancies support the contention that  $\text{CO}_2$  evasion alone could not explain the observed patterns in stream water  $\delta^{13}\text{C}_{\text{DIC}}$  values in this headwater catchment. While hillside groundwater  $\delta^{13}\text{C}_{\text{DIC}}$  values could be explained by the combined influence of terrestrial biogenic DIC sources followed by atmospheric  $\text{CO}_2$  evasion, data from stream water  $\delta^{13}\text{C}_{\text{DIC}}$  could suggest an additional contribution of in-stream DOC mineralization. These different processes can be separated and further quantified using the patterns in  $\delta^{13}\text{C}_{\text{DIC}}$  values. As defined by Amiotte-Suchet et al. (1999), Brunet et al. (2005, 2009) and Campeau et al. (2017), the range in  $\delta^{13}\text{C}_{\text{DIC}}$  observed in this study incorporated the three DIC end-members which are biogenic and geogenic sources and atmospheric  $\text{CO}_2$ . However, studies on the geochemistry of the NSEW have not identified the presence of carbonate minerals (Braun et al. 2005, 2012). As such positive  $\delta^{13}\text{C}_{\text{DIC}}$  value above  $-12\%$  assumed to indicate a certain degree of geogenic DIC influence (Deines et al. 1974) observed in groundwater from hillside could be interpreted as gas exchange across the soil-atmosphere interface, since deep penetration of atmospheric  $\text{CO}_2$  in these poor DOC groundwater could be associated with more positive  $\delta^{13}\text{C}_{\text{DIC}}$  values (Cerling et al. 1991; Davidson 1995; Liang et al. 2016). The importance of atmospheric DIC sources in hillside groundwater was further supported by the relationship between the calculated  $\text{CO}_2/\text{alkalinity}$  versus  $\delta^{13}\text{C}_{\text{DIC}}$ , plotted on theoretical  $\delta^{13}\text{C}_{\text{CO}_2}$  equilibrium lines, calculated according to Amiotte-Suchet et al. (1999) (Fig. 9a) and the relationship between the calculated  $\text{pCO}_2$  versus  $\delta^{13}\text{C}_{\text{DIC}}$  (Fig. 9b). Theoretical  $\delta^{13}\text{C}_{\text{CO}_2}$  trajectories

**Fig. 7**  $\delta^{13}\text{C}_{\text{DOC}}$  versus  $1/\text{DOC}$  in stream water and spring water (microbial biodegradation and DOC fixation on silt leads to the decreases in DOC and increases of  $\delta^{13}\text{C}_{\text{DOC}}$  in spring water)





showing  $\delta^{13}\text{C}_{\text{DIC}}$  values in equilibrium with both biogenic and atmospheric  $\text{CO}_2$  demonstrated a shift in DIC sources between these two end-members. Furthermore, in forested catchment on silicate basements, the  $\text{pCO}_2$  of the stream would be mainly controlled by the transformation between inorganic and organic forms of carbon (Wang et al. 2015; Zhong et al. 2018). This can be supported in the NSEW by the negative relationship between  $\text{pCO}_2$  and  $\delta^{13}\text{C}_{\text{DIC}}$  values (Fig. 9b), showing two main sources of carbon in this catchment which corroborates our interpretations of the approximated  $\text{CO}_2$  source from the Miller-Tans plot.

The significance of biogenic DIC sources was supported by the relationship between the calculated  $\text{pCO}_2$  values and DOC concentration across all sampling points (Fig. 10a) and the relationship between DOC concentration and  $\delta^{13}\text{C}_{\text{DIC}}$  values (Fig. 10b). This relationship is evident in rich DOC surface waters from the SLB and the stream, indicating that high DOC concentration could be related to the consistent  $\text{CO}_2$  oversaturation of the stream. The approximated stream water source of  $\delta^{13}\text{C}_{\text{DIC}}$  ( $-22.5\text{‰}$ ), demonstrated by the Miller-Tans analysis, represents a significant deviation from the isotopic composition of stream water DOC, although subject to a certain degree of uncertainty (median  $\delta^{13}\text{C}_{\text{DOC}} = -29.2\text{‰}$ ; Table 2b). This indicates that in-stream DOC mineralization was dominant but not likely the unique source of stream DIC. This contention was supported by the observation of poor DOC water with  $\text{CO}_2$  oversaturated (Log ( $\text{pCO}_2$ ) between  $-2.5$  and  $-2.0$ ; Fig. 10a) and low  $\delta^{13}\text{C}_{\text{DIC}}$  values from groundwater (Fig. 10b), which is instead more representative of soil respiratory  $\text{CO}_2$  (Liang et al. 2016; Campeau et al. 2017).

### 5.3 Response of Carbon to Hydrological Change

The ranges of variation of DIC and  $\delta^{13}\text{C}_{\text{DIC}}$  in groundwater were quite wide at low discharge, but drop considerably with increasing discharge (Fig. 11a, b showing DIC and  $\delta^{13}\text{C}_{\text{DIC}}$  versus discharge). The observed trend of increasing  $\delta^{13}\text{C}_{\text{DIC}}$  accompanied by decrease in groundwater DIC with increasing discharge supports the shift in DIC source within the hydrological cycle. It can be noted for spring water and groundwater that during

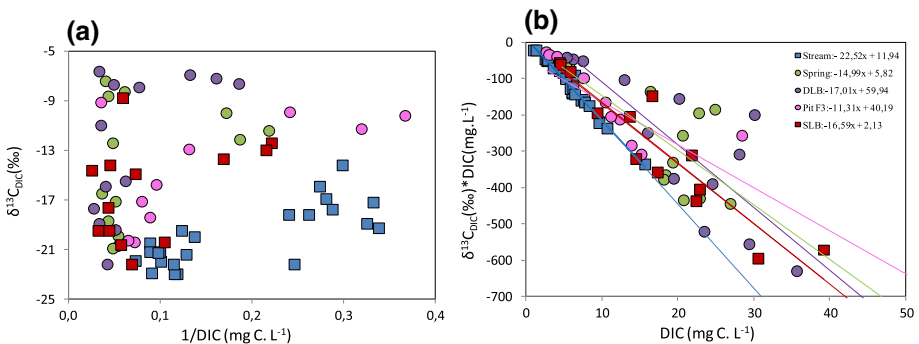


**Fig. 8** Keeling plot and Miller-Tans plot analysis for  $\delta^{13}\text{C}_{\text{DIC}}$  values (a, b). The Keeling plots (a) show the relationship between  $\delta^{13}\text{C}$  values as a function of  $1/\text{C}$ , while the Miller-Tans plots (b) present the relationship between  $\delta^{13}\text{C}_{\text{DIC}} \times \text{DIC}$  as a function of DIC. The regression lines are plotted for each individual sampling point with the equations listed in the legend

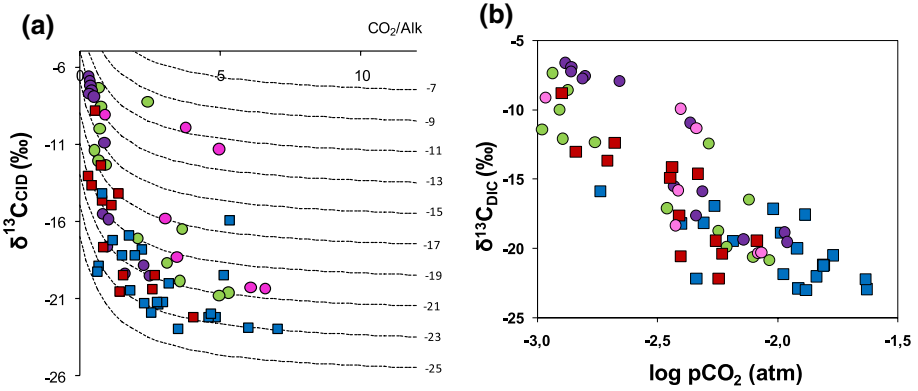


**Fig. 9** Evolution of  $\delta^{13}\text{C}_{\text{DIC}}$  versus  $\text{CO}_2/\text{alkalinity}$  ratio, compared to theoretical  $\delta^{13}\text{C}_{\text{CO}_2}$  equilibrium lines (shaded lines) (a) and relationship of  $\delta^{13}\text{C}_{\text{DIC}}$  versus  $\log(p\text{CO}_2)$  (b) showing the equilibrium of  $\delta^{13}\text{C}_{\text{DIC}}$  between two sources end-members (biogenic and atmospheric sources)

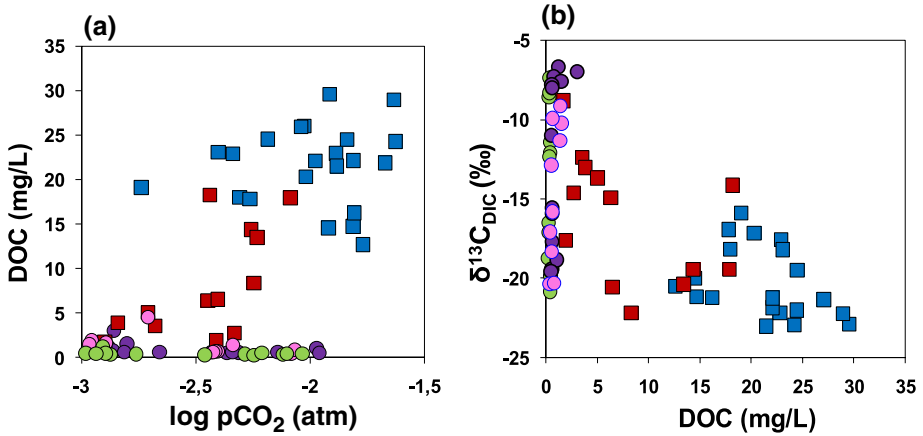


**Fig. 10** DOC (mg/L) versus  $\log p\text{CO}_2$  (atm) (a) and  $\delta^{13}\text{C}_{\text{DIC}}$  (‰) versus DOC (mg/L) (b) in soil waters and stream water, showing the dominance of DOC controls on  $\delta^{13}\text{C}_{\text{DIC}}$  and  $\log p\text{CO}_2$  in stream water

the SRS, SDS and LDS,  $\delta^{13}\text{C}_{\text{DIC}}$  ( $-6$  to  $-22\text{‰}$ ) seems to be in equilibrium with both  $^{13}\text{C}$  depleted gaseous  $\text{CO}_2$  and  $^{13}\text{C}$ -enriched gaseous  $\text{CO}_2$ . During the LRS,  $\delta^{13}\text{C}_{\text{DIC}}$  of groundwater gets closer to equilibrate only with  $^{13}\text{C}$ -enriched gaseous  $\text{CO}_2$ . This result suggests that both soils respiratory  $\text{CO}_2$  from which low  $\delta^{13}\text{C}$  values are derived and atmospheric  $\text{CO}_2$  invasion from which high  $\delta^{13}\text{C}$  values are obtained should be driven by seasonal water changes. The influence of soil-respired  $\text{CO}_2$  declines gradually with increasing drainage at the beginning of the SRS and during the LRS, leading to low DIC concentration and high  $\delta^{13}\text{C}$  values. This observation, described here for the first time, can be considered typical of humid tropical areas. Molecular diffusion of atmospheric gaseous  $\text{CO}_2$  through the soil pores (Cerling et al. 1991; Atekwana and Krishnamurthy 1998; Marx et al. 2017) and mineralization of soil organic matter are competitive and quite pronounced in the dry seasons, leading to a wide range of  $\delta^{13}\text{C}_{\text{DIC}}$ . During the rainy seasons, the saturation of the soil pores limits soil respiration and diffusion of gaseous  $\text{CO}_2$ ; thus, DIC is mainly brought by

dissolved atmospheric CO<sub>2</sub> in rainwater. As a result, the  $\delta^{13}\text{C}_{\text{DIC}}$  values were high, above the range of that of dissolved atmospheric CO<sub>2</sub> (Wang et al. 2015). Although the range of stream water DIC and  $\delta^{13}\text{C}_{\text{DIC}}$  were quite close with regard to groundwater, seasonal variations of the  $\delta^{13}\text{C}_{\text{DIC}}$  and DIC in the stream at the outlet of the catchment were observed, showing slight decreases in the  $\delta^{13}\text{C}_{\text{DIC}}$  that accompanied the decreases in groundwater DIC with increasing discharge (Fig. 11c, d). Given that the measured stream  $\delta^{13}\text{C}_{\text{DIC}}$  values were more <sup>13</sup>C-depleted, it is likely that biologically sourced carbon (probably from the turnover of wetland soil-sourced or in situ aquatic organic matter) mainly contributes to the riverine DIC pool. Though such biological influences are less pronounced during the rainy seasons due to the saturation of wetland soil, the shrinkage of swamps within the dry seasons may have increased soil respiration, leading to the observed <sup>13</sup>C-depleted values. These processes that controlled the carbon pools in the different water sources which contribute to the stream flow, could be explained using the hydrological model of the catchment described by Maréchal et al. (2011). According to this study, stream water comes mainly from (1) the surface flow from the swamp during storm events, (2) the subsurface groundwater flow from the swamp and (3) the seepage from hillside soil and bedrock. During the dry seasons (SDS and LDS), the swamp shrinks, promoting soil respiration and the diffusion of gaseous atmospheric CO<sub>2</sub> to a lesser extent. At this time, stream water is mainly supplied by discharge from the hillside aquifer, which flows through the swampy area, being subsequently enriched in organic carbon on contact with rich organic soils. As a result, stream  $\delta^{13}\text{C}_{\text{DIC}}$  equilibrates with respired CO<sub>2</sub> (Zhong et al. 2018). During the

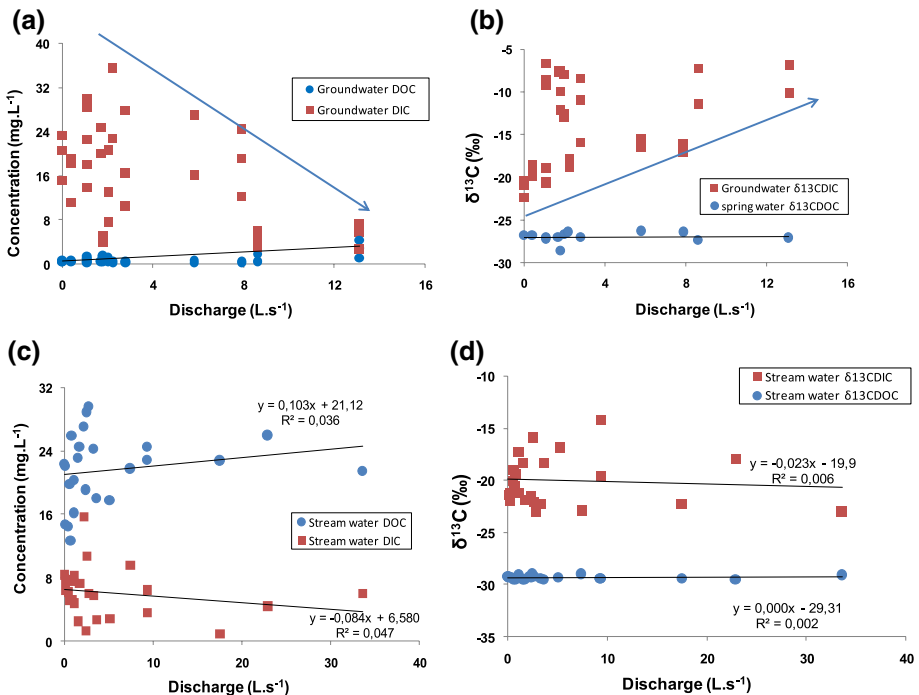


**Fig. 11** Cross plots of concentration versus river discharge (a, c) and  $\delta^{13}\text{C}$  versus river discharge (b, d) for groundwater and stream water of the NSEW

rainy seasons (SRS and LRS), stream water is supplied by surface and subsurface groundwater flow from the swamp. The saturation of this area limits soil respiration and the diffusion of gaseous atmospheric CO<sub>2</sub>. As reported by Lee et al. (2017), the corresponding mechanism of the resulting <sup>13</sup>C-depleted DIC in the stream water could be the accumulation of dissolved organic matter that was subsequently discharged to the river and then transformed into DIC through in-stream DOC oxidation. This explanation could be supported by the positive relationship between DOC concentration and discharge. This is consistent with a flushing of the DOC and POC in the uppermost soil horizons of the wetland zones, thus indicating that overland and soil flows are important sources of riverine DOC and POC during precipitation events and resulting high runoff (Wilson et al. 2013). In fact, as reported in many other catchments (Inamdar and Mitchell 2006; Sanderman et al. 2009; Lambert et al. 2011), the isotopic record provides good support of this mechanism since the wetland upper soil horizons are the only catchment DOC reservoirs with sufficiently negative δ<sup>13</sup>C<sub>DOC</sub> to account for the decrease in stream δ<sup>13</sup>C<sub>DOC</sub> values during the rise in water level.

## 6 Conclusion

In this study, we presented a comparative data set of soil δ<sup>13</sup>C<sub>TOC</sub> to stream water, soil water and groundwater δ<sup>13</sup>C<sub>DOC</sub>, δ<sup>13</sup>C<sub>POC</sub> and δ<sup>13</sup>C<sub>DIC</sub> values, highlighting their potential to trace both carbon sources and processes with seasonal water changes in a tropical headwater catchment with contrasting soil systems and water pathways. Stream δ<sup>13</sup>C<sub>DOC</sub> and δ<sup>13</sup>C<sub>POC</sub> were comparable and more depleted than spring water δ<sup>13</sup>C<sub>DOC</sub>, without showing any remarkable shift as the hydrological conditions changed, reflecting a unique SOC source and indicating that processes that converted SOC to DOC were distinct in both hillslope and wetland soils. Although hillslopes represent more than 20% of the catchment surface area, the swamp zones appear to be the main source area of the stream DOC, from which a great proportion of DIC is derived through in-stream mineralization. This is consistent with a flushing model whereby the rise in water table caused by rainfall enhances the surface flow into the uppermost soil horizons of the wetland swamp zone, which represents the predominant DOC and POC reservoir at the catchment scale. We demonstrated that the export of DIC from soil to stream results in CO<sub>2</sub> evasion to the atmosphere, with additional DIC sources from in-stream mineralization of DOC and molecular diffusion of gaseous CO<sub>2</sub>. These processes which are driven by seasonal water changes play a considerable role in the catchment DIC budget, as interpreted from their imprint on stream water and groundwater δ<sup>13</sup>C<sub>DIC</sub> values. The stream water and groundwater δ<sup>13</sup>C<sub>DIC</sub> values reported here have revealed distinct patterns, highlighting the rich complexity of biogeochemical processes controlling soil–stream carbon linkages, demonstrating that wetland soils are the dominant source of stream carbon during storms in this catchment. The result of this study shows that the swamp wetland zones play a so far underestimated role in the global estimates of the carbon cycle.

**Acknowledgements** The long-term monitoring on Nsimi Small Environmental Watershed (NSEW), is supported by the project titled, Observatoire de Recherche en Environnement-Basins Versants Expérimentaux Tropicaux (ORE/BVET); <http://bvvet.omp.obs-mip.fr>, where hydrological data and some geochemical data are available. We thank the team of the Nsimi Small Experimental Watershed (Nsimi SEW) and the Hydrological Research Centre (CRH) of Yaounde for setting up the NSEW and the Nyong hydrological network and for maintaining it. We also thank late Mathieu Zang and Mathurin Amougou of Nsimi village, Justin

Nlozoa and late Jean Pierre Bedimo Bedimo of CRH for their help and especially for the support during the sampling phase. We thank Lagane Clarisse for assistance with the analytical work at the "Géoscience Environnement Toulouse (GET)." This work was supported by a grant from the Service de Coopération et d'Action Culturelle of the French Embassy (SCAC-Yaoundé).

## References

- Amiotte-Suchet P, Auber D, Probst J-L, Gauthier-Lafaye F, Probst A, Andreux F, Viville D (1999)  $\delta^{13}\text{C}$  pattern of dissolved inorganic carbon in a small granitic catchment: the Strengbach case study (Vosges mountain, France). *Chem Geol* 159:129–145
- Amiotte-Suchet P, Linglois N, Leveque J, Andreux F (2007)  $^{13}\text{C}$  composition of dissolved organic carbon in upland forested catchments of the Morvan mountains (France): influence of coniferous and deciduous vegetation. *J Hydrol* 335:354–363
- Amundson R, Stern L, Baisden T, Wang Y (1998) The isotopic composition of soil and soil-respired  $\text{CO}_2$ . *Geoderma* 82(1–3):83–114
- Andersson JO, Nyberg L (2008) Spatial variation of wetlands and flux of dissolved organic carbon in boreal headwater streams. *Hydrol Process* 22(12):1965–1975
- Atekwana EA, Krishnamurthy RV (1998) Seasonal variations of dissolved inorganic carbon and  $\delta^{13}\text{C}$  of surface waters: application of a modified gas evolution technique. *J Hydrol* 205:265–278
- Balakrishna K, Probst J-L (2005) Organic carbon transport and C/N ratio variation in a large tropical river: Godavari as a case study, India. *Biogeochemistry* 73:457–473
- Balesdent J, Mariotti A (1996) Measurement of soil organic matter turnover using  $^{13}\text{C}$  natural abundances. In: Boutton TW, Yamasakieds SI (eds) *Mass spectrometry of soils*. Marcel Dekker Inc., New York, pp 83–111
- Bengtson P, Bengtsson G (2007) Rapid turnover of DOC in temperate forests accounts for increased  $\text{CO}_2$  production at elevated temperatures. *Ecol Lett* 10(9):783–790
- Billett MF, Deacon CM, Palmer SM, Dawson JJC, Hope D (2006) Connecting organic carbon in stream water and soils in a peatland catchment. *J Geophys Res* 111:G02010
- Bird MI, Giresse P, Ngos S (1998) A seasonal cycle in the carbon-isotope composition of organic carbon in the Sanaga River, Cameroon. *Limnol Oceanogr* 43:143–146
- Boeglin J-L, Ndam J-R, Braun J-J (2003) Composition of the different reservoir waters in a tropical humid area: example of the Nsimi catchment (Southern Cameroon). *J Afr Earth Sci* 37:103–110
- Boeglin J-L, Ndam Ngoupayou JR, Nyeck B, Etcheber H, Mortatti J, Braun J-J (2005) Soil carbon stock and river carbon fluxes in a humid tropical environment: the Nyong river basin (South Cameroon). In: Roose E, Lal R, Feller C, Barthès B, Stewart B (eds) *Advances in soil science*, vol 18. CRC Publisher, Boca Raton, pp 275–288
- Braun J-J, Ndam JR, Viers J, Dupré B, Bedimo Bedimo JP, Boeglin J-L, Sigha NL, Freyrier R, Robain H, Nyeck B, Rouiller J, Muller JP (2005) Present weathering rates in a humid tropical watershed: Nsimi, South Cameroon. *Geochim Cosmochim Acta* 69(2):357–387
- Braun J-J, Maréchal J-C, Riotte J, Boeglin J-L, Bedimo Bedimo J-P, Ndam Ngoupayou JR, Nyeck B, Robain H, Sekhar M, Audry S, Viers J (2012) Elemental weathering fluxes and saprolite production rate in a Central African lateritic terrain (Nsimi, South Cameroon). *Geochim Cosmochim Acta* 99:243–270
- Brunet F, Gaiero D, Probst J-L, Depetris PJ, Gauthier LF, Stille P (2005)  $\delta^{13}\text{C}$  tracing of dissolved inorganic carbon sources in Patagonian rivers (Argentina). *Hydrol Process* 19(17):3321–3344
- Brunet F, Dubois K, Veizer J, Nkoue Ndong GR, Ndam Ngoupayou JR, Boeglin JL, Probst J-L (2009) Terrestrial and fluvial carbon fluxes in a tropical watershed: Nyong basin, Cameroon. *Chem Geol* 265:563–572
- Campeau A, Wallin MB, Giesler R, Lofgren S, Morth CM, Schiff S, Venkiteswaran JJ, Bishop K (2017) Multiple sources and sinks of dissolved inorganic carbon across Swedish streams, refocusing the lens of stable C isotopes. *Sci Rep* 7(1):9158
- Campeau A, Bishop K, Nilsson MB, Klemmedtsson L, Laudon H, Leith FI, Öquist M, Wallin MB (2018) Stable carbon isotopes reveal soil-stream DIC linkages in contrasting headwater catchments. *J Geophys Res Biogeosci*. <https://doi.org/10.1002/2017JG004083>
- Caroni R, Free G, Visconti A, Manca M (2012) Phytoplankton functional traits and seston stable isotopes signature: a functional-based approach in a deep, subalpine lake, Lake Maggiore (N. Italy). *J Limnol* 71(1):84–94


- Cerling TE, Solomon DK, Quade J, Bowman JR (1991) On isotopic composition of carbon in soil carbon dioxide. *Geochim Cosmochim Acta* 55:3403–3405
- Coyne A, Seyler P, Etcheber H, Meybeck M, Orange D (2005) Spatial and seasonal dynamics of total suspended sediment and organic carbon species in the Congo River. *Glob Biogeochem Cycles* 19(4):GB4019
- Craig H (1957) The natural distribution of radiocarbon and the exchange time of carbon dioxide between atmosphere and sea. *Tellus* 9(1):1–17
- Crawford JT, Lottig NR, Stanley EH, Walker JF, Hanson PC, Finlay JC, Striegl RG (2014) CO<sub>2</sub> and CH<sub>4</sub> emissions from streams in a lake-rich landscape: patterns, controls, and regional significance. *Glob Biogeochem Cycles* 28:197–210
- Davidson GR (1995) The stable isotopic composition and measurement of carbon in soil CO<sub>2</sub>. *Geochim Cosmochim Acta* 59(12):2485–2489
- Day FP, West SK, Tupacz EG (1988) The influence of ground-water dynamics in a periodically flooded ecosystem, the Great Dismal Swamp. *Wetlands* 8:1–13
- Deines P, Langmuir D, Harmon RS (1974) Stable carbon isotope ratios and the existence of a gas phase in the evolution of carbonate ground waters. *Geochim Cosmochim Acta* 38(7):1147–1164
- Dickson AG, Sabine CL, Christian JR (2007) Guide to best practices for ocean CO<sub>2</sub> measurements, vol 3. North Pacific Marine Science Organization, Sidney, pp 3–13
- Diochon A, Kellman L (2008) Natural abundance measurements of <sup>13</sup>C indicate increased deep soil carbon mineralization after forest disturbance. *Geophys Res Lett* 35:L14402
- Doctor DH, Kendall C, Sebestyen SD, Shanley JB, Ote N, Boyer EW (2008) Carbon isotope fractionation of dissolved inorganic carbon (DIC) due to outgassing of carbon dioxide from a headwater stream. *Hydrol Process* 22(14):2410–2423
- Evans CD, Freeman C, Cork LG, Thomas DN, Reynolds B, Billett MF, Garnett MH, Norris D (2007) Evidence against recent climate-induced destabilisation of soil carbon from C-14 analysis of riverine dissolved organic matter. *Geophys Res Lett* 34:L07407
- Feller C, Beare MH (1997) Physical control of soil organic matter dynamics in the tropics. *Geoderma* 79:69–116
- Gao Q, Tao Z, Yao G, Ding J, Liu Z, Liu K (2007) Elemental and isotopic signatures of particulate organic carbon in the Zengjiang River, southern China. *Hydrol Process* 21:1318–1327
- Hotchkiss ER, Hall RO, Sponseller RA, Butman D, Klaminder J, Laudon H, Rosvall M, Karlsson J (2015) Sources of and processes controlling CO<sub>2</sub> emissions change with the size of streams and rivers. *Nat Geosci* 8(9):696–699
- Huang W, McDowell WH, Zou X, Ruan H, Wang J, Li L (2013) Dissolved organic carbon in headwater streams and riparian soil organic carbon along an altitudinal gradient in the Wuyi mountains, China. *PLoS One* 8(11):e78973
- Inamdar SP, Mitchell MJ (2006) Hydrologic and topographic controls on stormevent exports of dissolved organic carbon (DOC) and nitrate across catchment scales. *Water Resour Res* 42:W03421
- Keeling CD (1958) The concentration and isotopic abundances of atmospheric carbon dioxide in rural areas. *Geochim Cosmochim Acta* 13(4):322–334
- Koutika L-S, Bartoli F, Andreux F, Cerri CC, Burtin G, Choné T, Philippy R (1997) Organic matter dynamics and aggregation in soils under rain forest and pastures of increasing age in the eastern Amazon Basin. *Geoderma* 76:87–112
- Kroopnick PM, Deuser WG, Graig H (1970) Carbon-13 measurements on dissolved inorganic carbon in the North Pacific (1969) GEOSECS station. *J Geophys Res* 75:7668–7671
- Krüger JP, Leifeld J, Alewell C (2014) Degradation changes stable carbon isotope depth profiles in peatlands. *Biogeosciences* 11:3369–3380
- Lambert T, Pierson-Wickmann A-C, Gruau G, Thibault JN, Jaffrezic A (2011) Carbon isotopes as tracers of dissolved organic carbon sources and water pathways in headwater catchments. *J Hydrol* 402:228–238
- Lambert T, Pierson-Wickmann A-C, Gruau G, Jaffrezic A, Petitjean P, Thibault JN, Jeanneau L (2014) DOC sources and DOC transport pathways in a small headwater catchment as revealed by carbon isotope fluctuation during storm events. *Biogeosciences* 11:3043–3056
- Lapierre JF, Guillemette F, Berggren M, del Giorgio PA (2013) Increases in terrestrially derived carbon stimulate organic carbon processing and CO<sub>2</sub> emissions in boreal aquatic ecosystems. *Nat Commun* 4:1–7
- Lauerwald R, Hartmann J, Ludwig W, Moosdorf N (2012) Assessing the nonconservative fluvial fluxes of dissolved organic carbon in North America. *J Geophys Res* 117:G01027

- Ledesma JIJ, Futter MN, Blackburn M, Lidman F, Grabs T, Sponseller RA, Laudon H, Bishop KH, Köhler SJ (2017) Towards an improved conceptualization of riparian zones in boreal forest headwaters. *Ecosystems* 21:1–19
- Lee KY, van Geldern R, Barth JAC (2017) A high-resolution carbon balance in a small temperate catchment: insights from the Schwabach River, Germany. *Appl Geochem* 85:86–96
- Leith FI, Dinsmore KJ, Wallin MB, Billett MF, Heal KV, Laudon H, Öquist MG, Bishop K (2015) Carbon dioxide transport across the hillslope-riparian-stream continuum in a boreal headwater catchment. *Biogeosciences* 12(6):1881–1892
- Liang LL, Riveros-Iregui DA, Risk DA (2016) Spatial and seasonal variabilities of the stable carbon isotope composition of soil CO<sub>2</sub> concentration and flux in complex terrain. *J Geophys Res Biogeosci* 121:2328–2339
- Ludwig W, Probst J-L, Kempe S (1996) Predicting the oceanic input of organic carbon by continental erosion. *Glob Biogeochem Cycles* 10:23–41
- Maréchal J-C, Braun J-J, Riotte J, Bedimo Bedimo J-P, Boeglin J-L (2011) Hydrologic processes of a rain-forest headwater swamp from natural chemical tracing in Nsimi watershed, Cameroon. *Hydrol Process* 25:2246–2260
- Marx AJ, Dusek J, Jankovec M, Sanda T, Vogel R, van Geldern J, Hartmann J, Barth JAC (2017) A review of CO<sub>2</sub> and associated carbon dynamics in headwater streams: a global perspective. *Rev Geophys* 55:560–585
- Maurizot P, Abessolo A, Feybesse JL, Johan V, Lecomte P (1986) Etude et Prospection Minière du Sud-Ouest Cameroun-Synthèse des Travaux de 1978 à 1985. BRGM, Direction des Activités Minières, Orléans
- Mayorga E, Aufdenkampe AK, Masiello CA, Krusche AV, Hedges JJ, Quay PD, Richey JE, Brown TA (2005) Young organic matter as a source of carbon dioxide outgassing from Amazonian rivers. *Nature* 436(7050):538–541
- Miller JB, Tans PP (2003) Calculating isotopic fractionation from atmospheric measurements at various scales. *Tellus B* 55(2):207–214
- Morel B, Durand P, Jaffeze A, Gruau G, Molénat J (2009) Sources of dissolved organic carbon during stormflow in a headwater agricultural catchment. *Hydrol Process* 23:2888–2901
- Ndam JR (1997) Bilans hydrogéo-chimiques sous forêt tropicale humide en Afrique: du bassin expérimental de Nsimi-Zoétélé aux réseaux hydrographiques du Nyong et de la Sanaga au Sud-Cameroun. Ph.D. dissertation, University Pierre et Marie Curie Paris VI
- Ndam Ngoupayou JR, Nkoue Ndondo GR, Boeglin JL, Braun JJ, Kamgang Kabeyene VB, Ekodeck GE (2005a) Water and fluxes of matter transfers during a storm event in the Mengong experimental watershed (Nsimi-South Cameroon). In: Heathwaite AL (ed) Dynamics and biogeochemistry of river corridors and wetlands, vol 294. IAHS Publications, Wallingford, pp 183–190
- Ndam Ngoupayou JR, Boeglin J-L, Probst J-L, Braun J-J, Meybeck M, Nkoue Ndondo GR (2005b) The organic carbon dynamics of a small catchment in the humid tropics. In: Walling DE, Horowitz AJ (eds) Sediment budgets 1, vol 291. IAHS Publications, Foz do Iguacu, pp 46–53
- Nelson PN, Baldock JA, Oades JM (1993) Concentration and composition of dissolved organic carbon in streams in relation to catchment soil properties. *Biogeochemistry* 19:27–50
- Ngao J, Cotrufo MF (2011) Carbon isotope discrimination during litter decomposition can be explained by selective use of substrate with differing  $\delta^{13}\text{C}$ . *Biogeosci Discuss* 8:51–82
- Nier AO (1950) A redetermination of the relative abundances of the isotopes of carbon, nitrogen, oxygen, argon, and potassium. *Phys Rev* 77:789–793
- Nkoue Ndondo G (2008) Le cycle du carbone en domaine tropical humide : exemple du bassin versant forestier du Nyong au sud Cameroun. Thesis (Ph.D.), University of Toulouse 3
- Olivia P, Viers J, Dupré B, Fortune JP, Martin F, Braun JJ, Nahon D, Robain H (1999) The effect of organic matter on chemical weathering: study of a small tropical watershed: Nsimi-Zoetele site, Cameroon. *Geochim Cosmochim Acta* 63:4013–4035
- Olivie-Lauquet G, Allard T, Benedetti M, Muller J-P (1999) Chemical distribution of trivalent iron in riverine material from a tropical ecosystem: a quantitative EPR study. *Water Res* 33:2726–2734
- Olivie-Lauquet G, Allard T, Bertaux J, Muller JP (2000) Crystal-chemistry of suspended matter in a tropical hydrosystem: Nyong basin (Cameroon, Africa). *Chem Geol* 170:113–131
- Opsahl SP, Zepp RG (2001) Photochemically-induced alteration of stable carbon isotope ratios ( $\delta^{13}\text{C}$ ) in terrigenous dissolved organic carbon. *Geophys Res Lett* 28(12):2417–2420
- Öquist MG, Wallin M, Seibert J, Bishop K, Laudon H (2009) Dissolved inorganic carbon export across the soil/stream interface and its fate in a boreal headwater stream. *Environ Sci Technol* 43(19):7364–7369
- Palmer SM, Hope D, Billett MF, Dawson JJC, Bryant CL (2001) Sources of organic and inorganic carbon in a headwater stream: evidence from carbon isotope studies. *Biogeochemistry* 52(3):321–338



- Polsenaere P, Abril G (2012) Modelling CO<sub>2</sub> degassing from small acidic rivers using water pCO<sub>2</sub>, DIC and δ<sup>13</sup>C<sub>DIC</sub> data. *Geochim Cosmochim Acta* 91:220–239
- Porcal P, Dillon PJ, Molot LA (2015) Temperature dependence of photodegradation of dissolved organic matter to dissolved inorganic carbon and particulate organic carbon. *PLoS One* 10(6):e0128884
- Powers JS, Schlesinger WH (2002) Geographic and vertical patterns of stable carbon isotopes in tropical rain forest soils of Costa Rica. *Geoderma* 109:141–160
- Probst J-L, Mortatti J, Tardy Y (1994) Carbon river fluxes and weathering CO<sub>2</sub> consumption in the Congo and Amazon river basins. *Appl Geochem* 9:1–13
- Richey JE, Melack JM, Aufdenkampe AK, Ballester VM, Hess LL (2002) Outgassing from Amazonian rivers and wetlands as a large tropical source of atmospheric CO<sub>2</sub>. *Nature* 416:617–620
- Sanderman J, Baldock JA, Amundson R (2008) Dissolved organic carbon chemistry and dynamics in contrasting forest and grassland soils. *Biogeochemistry* 89:181–198
- Sanderman J, Lohse KA, Baldock JA, Amundson R (2009) Linking soils and streams: sources and chemistry of dissolved organic matter in a small coastal watershed. *Water Resour Res* 45(3):W03418
- Shin WJ, Chung GS, Lee D, Lee KS (2011) Dissolved inorganic carbon export from carbonate and silicate catchments estimated from carbonate chemistry and δ<sup>13</sup>C<sub>DIC</sub>. *Hydrol Earth Syst Sci* 15:2551–2560
- Strohmeier S, Knorr KH, Reichert M, Frei S, Fleckenstein JH, Peiffer S, Matzner E (2013) Concentrations and fluxes of dissolved organic carbon in runoff from a forested catchment: insights from high frequency measurements. *Biogeosciences* 10(2):905–916
- Takam T, Arima M, Kokonyangi J, Dunkley DJ, Nsifa EN (2009) Paleoproterozoic charnockite in the Nten Complex, Congo Craton, Cameroon: insights from SHRIMP zircon U-Pd ages. *J Miner Pet Sci* 104:1–11
- Telmer K, Veizer J (1999) Carbon fluxes, pCO<sub>2</sub> and substrate weathering in a large northern river basin, Canada: carbon isotope perspectives. *Chem Geol* 159(1–4):61–86
- Venkiteswaran JJ, Schiff SL, Wallin MB (2014) Large carbon dioxide fluxes from headwater boreal and sub-boreal streams. *PLoS One* 9(7):e101756
- Viers J, Dupré B, Polvé M, Schott J, Dandurand JL, Braun JJ (1997) Chemical weathering in the drainage basin of a tropical watershed (Nsimi-Zoetele site, Cameroon): comparison between organic poor and organic rich waters. *Chem Geol* 140:181–206
- Viers J, Dupré B, Braun J-J, Deberdt S, Angeletti B, Ngoupayou JN, Michard A (2000) Major and trace element abundances and strontium isotopes in the Nyong basin rivers (Cameroon): constraints on chemical weathering processes and elements transport mechanisms in humid tropical environments. *Chem Geol* 169:211–241
- Viers J, Dupré B, Braun JJ, Freydisier R, Greenberg S, Ndam Ngoupayou JR, Sigha Nkamdjou L (2001) Evidence for nonconservative behavior of chlorine in humid tropical environments. *Aquat Geochem* 7:127–154
- Wallin MB, Grabs T, Buffam I, Laudon H, Agren A, Oquist MG, Bishop K (2013) Evasion of CO<sub>2</sub> from streams—the dominant component of the carbon export through the aquatic conduit in a boreal landscape. *Glob Change Biol* 19(3):785–797
- Wang FS, Cao M, Wang BL, Fu JA, Luo WY, Ma J (2015) Seasonal variation of CO<sub>2</sub> diffusion flux from a large subtropical reservoir in East China. *Atmos Environ* 103:129–137
- Weiss RF (1974) Carbon dioxide in water and seawater: the solubility of non-ideal gas. *Mar Chem* 2:203–215
- Wilson HF, Saiers JE, Raymond PA, Sobczak WV (2013) Hydrologic drivers and seasonality of dissolved organic carbon concentration, nitrogen content, bioavailability, and export in a forested New England stream. *Ecosystems* 16(4):604–616
- Wynn JG, Bird MI (2007) C4-derived soil organic carbon decomposes faster than its C3 counterpart in mixed C3/C4 soils. *Glob Change Biol* 13(10):1–12
- Wynn JG, Harden JW, Fries TL (2006) Stable carbon isotope depth profiles and soil organic carbon dynamics in lower Mississippi Basin. *Geoderma* 131:89–109
- Zeebe RE, Wolf-Gladrow DA (2001) CO<sub>2</sub> in seawater: equilibrium, kinetics, isotopes, vol 65. Gulf Professional Publishing, Houston
- Zhang J (1995) Carbon isotope fractionation during gas–water exchange and dissolution of CO<sub>2</sub>. *Geochim Cosmochim Acta* 59(1):107–114
- Zhong J, Li S-L, Ding H, Lang Y, Maberly SC, Xu S (2018) Mechanisms controlling dissolved CO<sub>2</sub> oversaturation in the Three Gorges Reservoir area. *Inland Waters* 8(2):148–156

## Affiliations

**Gustave Raoul Nkoue Ndondo**<sup>1</sup>  · **J.-L. Probst**<sup>2</sup> · **J. Ndjama**<sup>4</sup> ·  
**Jules Remy Ndam Ngoupayou**<sup>5</sup> · **J.-L. Boeglin**<sup>3</sup> · **G. E. Takem**<sup>4</sup> · **F. Brunet**<sup>2</sup> · **J. Mortatti**<sup>6</sup> ·  
**F. Gauthier-Lafaye**<sup>7</sup> · **J.-J. Braun**<sup>3,4,8</sup> · **G. E. Ekodeck**<sup>5</sup>

- <sup>1</sup> Department of Earth Sciences, University of Douala, P.O. Box: 24157, Douala, Cameroon
- <sup>2</sup> Laboratoire d'Ecologie Fonctionnelle (EcoLab), Institut National Polytechnique de Toulouse (INPT), ENSAT, Université de Toulouse, Avenue de l'Agrobiopole, 31326 Castanet Tolosan Cedex, France
- <sup>3</sup> Géosciences Environnement Toulouse (GET-Université de Toulouse, CNRS, IRD), Université de Toulouse, 14 Avenue Edouard-Belin, 31400 Toulouse, France
- <sup>4</sup> Institut de Recherches Géologiques et Minières/Centre de Recherches Hydrologiques, BP 4110, Yaoundé, Cameroun
- <sup>5</sup> Department of Earth Sciences, University of Yaoundé I, P.O. Box: 812, Yaoundé, Cameroon
- <sup>6</sup> Centro de Energia Nuclear na Agricultura (CENA), University of Sao Paulo, Piracicaba, SP 13416-000, Brazil
- <sup>7</sup> Centre National de Recherche Scientifique (CNRS), Centre de Géochimie de la Surface (CGS), Université de Strasbourg, 1 Rue Blessig, CS 50007, 67084 Strasbourg Cedex, France
- <sup>8</sup> International Joint Laboratory DYCOFAC, IRGM-UY1-IRD, Rue Joseph Essono Balla, Quartier Elig Essono, BP 1857, Yaoundé, Cameroun